Journal of Materials Chemistry A

Accepted Manuscript

This article can be cited before page numbers have been issued, to do this please use: S. Yang, W. Fu, Z. Zhang, H. Chen and C. Li, *J. Mater. Chem. A*, 2017, DOI: 10.1039/C7TA00366H.

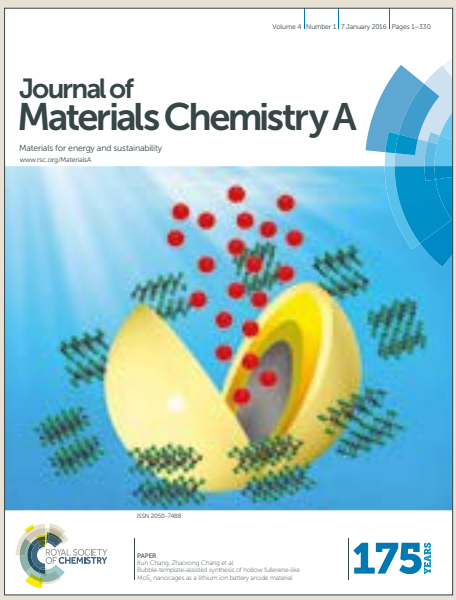

ROYAL SOCIETY OF CHEMISTRY

rsc.li/materials-a

View Article Online
DOI: 10.1039/C7TA00366H

Journal Name

ARTICLE

Recent Advances in Perovskite Solar Cells: Efficiency, Stability and Lead-free Perovskite

Received 00th January 20xx,
Accepted 00th January 20xx

DOI: 10.1039/x0xx00000x

www.rsc.org/

Shida Yang, Weifei Fu, Zhongqiang Zhang, Hongzheng Chen and Chang-Zhi Li*

With the rapid growth of efficiency from 3.8 % to 22.1 % in recent years, perovskite solar cells (PVSCs) have drawn great attentions of researchers from both academia and industry. However, it gives no doubt that significant barriers remain standing in the pathway of PVSC advancements. To deal with high-efficiency and stable devices, as well as environmentally benign perovskites are the critical, yet challenging aspects of PVSC research. In this review article, we focus on the recent advances of the related subjects. The approaches for high-efficiency PVSCs are introduced first and thenthe instability issues and lead-free perovskite are discussed. In the last, the conclusion along with brief perspectives are provided on further advancing PVSC toward efficient and stable solar-to-electricity technologies.

1. Introduction

Organic−inorganic hybrid lead halide perovskites attracted researcher's attentions during 1970s and 1990s,[1-4] especially for their unique semiconducting and conducting properties.[5-7] In 2009, the research efforts to apply lead perovskite as light absorbers into solar cells were deployed that Miyasaka *et al.* incorporated $CH_3NH_3PbI_3$ ($MAPbI_3$) and $CH_3NH_3PbBr_3$ ($MAPbBr_3$) as sensitizers into dye-sensitized solar cells (DSSCs), delivering the 3.8% and 3.1% power conversion efficiency (PCE), respectively.[8] In light of the major source of clean and sustainable energy on earth, solar flux has long been sought to convert into electricity through the photovoltaic effect of light-absorbing semiconductors. Earlier generation photovoltaics utilized inorganic crystalline semiconductors, such as silicon, cadmium telluride (CdTe) and copper indium gallium selenide/sulfide (CIGS) as absorbers, which can be efficient and stable, but usually requiring high energy-input manufacture, involving high-temperature and high-vacuum processes.

The emerging organic-inorganic hybrid perovskite solar cells (PVSCs) represent one of the transformative technologies, because they, like organic solar cells (OSCs)[9, 10] and DSSCs[11], potentially can be transited into light-weight, flexible and low-cost power sources through the high-throughput solution fabrication.[12] PVSCs have therefore acquired the intensive research efforts from both academia and industry. The PCEs of PVSCs have been rapidly improved from 3.8 % to 22.1 % in just seven years,[13] demonstrating the rivalry in efficiency to that of silicon solar cells. It essentially benefits from the exceptional optoelectrical properties of semiconducting organic–inorganic hybrid perovskites, such as the strong optical absorption coefficient, a direct band gap, long carrier life time and diffusion length[14-17] and high electron/hole mobility in crystalline state.[18, 19] More importantly, organic-inorganic lead halide perovskites generate loosely bonded exciton with really small bonding energy, which facilitates the generation of free charge carriers within the perovskite by the cost of minimal driving force.[20, 21]As a result, the rapid advancement of single junction PVSC has reached the level close to its theoretical efficiency ceiling, through the combined innovations on the elemental composition, crystalline film formation, interface and device architecture etc.[22-35]

Although the magnificent progresses were made for PVSCs, a number of barriers ranging from fundamental to practical still remain, which need to be further overcome to validate their commercial relevance, as those of traditional silicon solar cells. For instance, concerns on the operational stability of PVSC and environmentally benign perovskite composition need to be further addressed for pushing PVSC technology on a large scale.[36, 37] It is known that the $MAPbI_3$ perovskite is liable to degrade under the exposure to moisture, heat and prolonged illumination in air.[38] Therefore, the prototype PVSC possesses a relatively short operational lifetime upon exposure to humidity, heat and light. One prerequisite for market consideration is to extend the lifespan of PVSCs likely to decades at outdoor conditions. On the other hand, lead-based perovskites contain water soluble Pb salt as a degradation product, which is toxic upon human exposure.

Although these challenges pose barriers to PVSC advancement, the encouraging discoveries have been achieved in the recent 2-3 years for PVSCs. It gives no doubt that to deal with high-efficiency and stable devices, as well as environmentally benign perovskites are the critical, yet

*State Key Laboratory of Silicon Materials, MOE Key Laboratory of Macromolecular Synthesis and Functionalization, Department of Polymer Science and Engineering, Zhejiang University, Hangzhou 310027, P. R. China. *E-mail: czli@zju.edu.cn*

† Footnotes relating to the title and/or authors should appear here.

challenging aspects of PVSC research. Herein, we focus on the recent advances of PVSCs in the related subjects. In the following parts of this review article, we first introduce the approaches that enable high-efficiency PVSCs through the perovskite films processing, composition engineering, interfacial layer and tandem architecture. Then, the material and device stabilities, and the development of lead-free perovskite will be discussed. In the last section, we outline conclusions along with brief perspectives on further advancing PVSC toward efficient and stable solar-to-electricity technologies.

2. High-Efficiency Perovskite Solar Cells

High efficiency is one of the central criteria for validating the practical relevance of solar cells. The primary endeavour devoted to PVSC research is perhaps to obtain highly efficient devices. The PCE of solar cell is defined by short-circuit current density (*J*sc), open-circuit voltage (*V*oc), and fill factor (FF). Three parameters closely interplay with the quality of perovskite film and perovskite composition,[39-42] the interfacial contact,[43-46] as well as the device architecture[47-49]. Basically, the V_{OC} correlates to the quasi-Fermi level of photo-excited perovskite and the electrode work function. To obtain high J_{SC}, perovskite absorber needs to harvest incident photos completely, while maintaining efficient charge generation, transport and extraction with minimal recombination. FF relates to the parasitic series resistance (*Rs*) and shunt resistance (*Rp*) of devices,[50, 51] depending on the bulk conductivity of each layers, and the contact resistance in between. In this section, we introduce recent approaches led to high-efficiency PVSCs, including perovskite film processing, composition and interface engineering, as well as device architecture.

First of all, the widely used single junction PVSC architecture can be catalogued into mesoscopic and planar heterojunction structures **(Figure 1)**. In mesoscopic structure, a mesoporous metal oxide scaffold, such as titanium oxide (TiO_2) or aluminium oxide, (Al_2O_3) is applied, into which the perovskite is infiltrated.[24] On the other hand, benefited from the high ambipolar mobilities of perovskite, PVSC can also afford a planar heterojunction configuration instead, avoiding the harsh processing of mesoporous TiO_2. The planar devices include regular (n-i-p)[52] and inverted (p-i-n)[53] devices, depending on which selective contact is used atop of transparent electrode. It is worth to note that the current best performing devices usually reported with mesoscopic devices. Recently, the efficiencies for planar devices are also improved over 20%, whereas the fabrication of planer devices is relatively easier compared to that of TiO_2 based mesoporous devices.

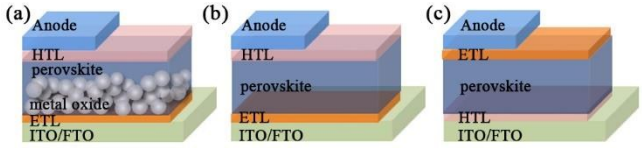

Figure 1. Device architectures of mesoporous, regular (n-i-p) and inverted (p-i-n) PVSCs.

2.1 Perovskite Films Processing

The evolution of device efficiencies requires the continuously improving the film quality of crystalline perovskite layers, to be uniform, smooth, and pin-hole free etc. Here, we exemplify several effective methodologies for the access of high quality thin film. Vapor-deposition method was introduced by Liu *et al.* to achieve an efficiency over 15% in planar heterojunction PVSCs (**Figure 2a**).[54] This method produces good uniformity of the perovskite films over a range of length scales, subsequently resulting in good performance. It also shows the advantage to prepare multi-stack thin films over large areas.[55] Solution fabrication is attractive for solar cell technology due to the merit of low energy-consumption at massive manufacture. However, the challenge is that perovskites are hard to form compact and flat films due to the strong tendency of anisotropic crystallization during solvent evaporation. Thus, fabrication strategies to control the rapid crystallization of such perovskites are necessary. Generally, to control the kinetics between nucleation and crystal grain growth is an effective way for obtaining high quality perovskite films with excellent optoelectronic properties.

Jeon *et al.* first reported the anti-solvent (solvent engineering) method to obtain high-quality perovskite film and figure out that DMSO is able to form an intermediate MAI-PbI_2-DMSO to retard the crystal growth of perovskite, which is extensively adopted by different research groups.[56-59] Chen *et al.* also developed a fast crystallization method involving spin coating of a DMF solution of $MAPbI_3$ followed by immediate exposure to chlorobenzene to promote perovskite film formation (**Figure 2b**). Later, a gas-assisted solution processing technique is developed, which delivers uniform perovskite films consisting of densely packed single crystalline grains.[60]

Two-step deposition is also proven to be efficient for achieving excellent films. Burschka *et al.* first developed a two-step method, in which PbI_2 was introduced onto a porous TiO_2 film and subsequently converted into the perovskite by exposing it to MAI solution, which yield perovskite film with improved film quality and increased the efficiency to 15% in mesoporous devices.[61] Afterwards, an interdiffusion method was introduced by Xiao *et al.*, which combines a sequence spin-coating of PbI_2 and MAI, then converting into perovskite film (**Figure 2c**), yielding 15.4% PCE in planar device.[62] Further combined with DMF solvent annealing, the quality of perovskite films from interdiffusion method can be further improved to reach high efficiency with a thickness of 630 nm in planar devices.[63] Very recently, Bi *et al.* demonstrated PMMA can template the nucleation and crystal growth of perovskite films with fewer defects and larger oriented grains, enabling perovskite solar cells to achieve a certified PCE of 21.02%.[64]

Although the highest certified PCE of PVSCs surpassed 22%, approaching the record PCEs of commercialized thin-film technologies based on CIGS or CdTe. It still shows far distance to the practical relevance since the fact that most high PCEs of PVSCs are recorded on small areas, typically around 0.1 cm^2. The PCEs of large area PVSCs still lag behind those of small area devices. One of the key challenges for up-scaling PVSCs

is the fabrication of pinhole-free, uniform perovskite films on large areas with high reproducibility.[65] Deng *et al.* used scalable doctor-blade coating to fabricate $MA_{0.6}FA_{0.4}PbI_3$ PVSCs, obtaining a high efficiency of 18.3% (**Figure 3a**).[66] It offers controlling freedom for film formation (e.g., temperature, precursor stoichiometry) to obtain high quality perovskite films, which can be a supplement to spin-coating method. Gu *et al.* applied roll-to-roll (R2R) coating to fabricated $MAPbI_{3-x}Cl_x$ film on SAM modified PEDOT:PSS and obtained an efficiency of 5.1% for the semi-R2R solar cell.[67] Schmidt *et al.* used slot-die coating to make $MAPbI_3$ on flexible PET/ITO. Combined with a printed back electrode, such fully roll processing flexible perovskite solar cell has an efficiency of 4.9%.[68] A vacuum flash–assisted solution process (VASP) (**Figure 3b**) is recently developed for high-efficiency large-area PVSCs. With shiny, smooth and crystalline perovskite films of high electronic quality over large areas, solar cells with an aperture area exceeding 1 cm^2 showing a maximum efficiency of 20.5% and a certified PCE of 19.6% was achieved.[42] Conings *et al.* invented the universal complex-assisted gas quenching (CAGQ) method, which introduces nitrogen gas flow to take away residue solvent to form an intermediate DMSO-complex, and applied it to many perovskite materials. Through this method, an efficiency of 18.0% was obtained (**Figure 3c**).[69] Ye *et al.* developed a soft-cover deposition (SCD) method (**Figure 3d**) to obtain pinhole-free, large crystal grains and rough-border-free $MAPbI_3$ perovskite films with large area up to 51 cm^2. This SCD method also improves the material utilization efficiency to ~80%, much higher than spin-coating (only 1%). A reproducible PCE of 17.6% is achieved for 1 cm^2 solar cells.[70]

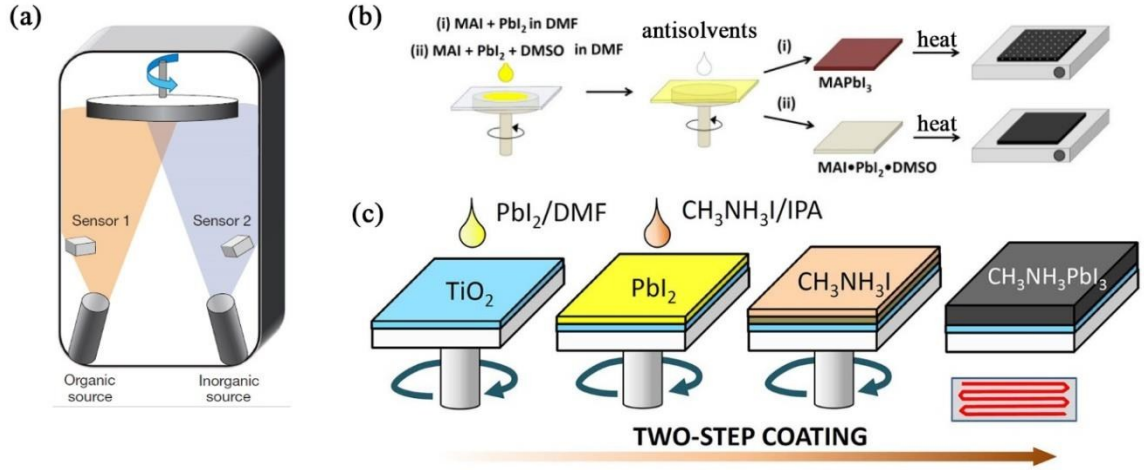

Figure 2 Summaries of different deposition methods for high quality perovskite films: (a) vapor deposition[54], (b) anti-solvents[71] and (c) two step methods[72]. Adapted with permission from ref. [54] Copyright 2013 Nature Publishing Group, from ref. [71] Copyright 2015 American Chemical Society, from ref. [72] Copyright 2015 The Royal Society of Chemistry.

View Article Online
DOI: 10.1039/C7TA00366H

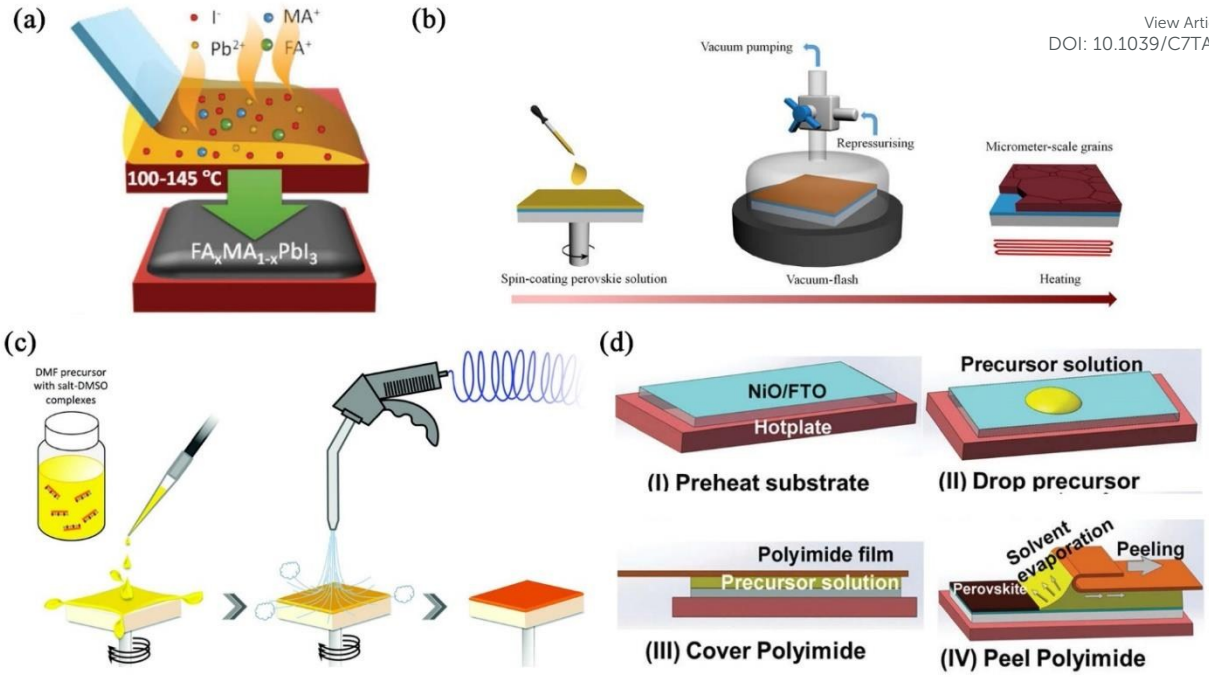

Figure 3 Schematic of potential scalable fabrication methods: (a) doctor-blade coating. [66] (b) VASP method. [42] (c) CAGQ method. [69] (d) SCD method.[70] Adapted with permission from ref. [66] and [69] Copyright 2016 Wiley-VCH Verlag GmbH & Co. KGaA, from ref. [42] Copyright 2016 American Association for the Advancement of Science, from ref. [70] Copyright 2016 The Royal Society of Chemistry.

Thanks to the sophisticated fabrication methods developed so far, the progress of device efficiencies is approaching its theoretical limitation in single junction PVSCs with small area. To push PVSC into real application, the continuous efforts are needed to fabricate high quality crystalline perovskite film into large area with good reproducibility.

2.2 Composition Engineering

Regarding to the general formula of ABX_3, perovskites for solar cells application usually contain A of a monovalent cation, a divalent cation B, and a monovalent anion X.[73] The choices of component ions not only determine crystal unit structure, but also tune the optoelectrical properties of the resultant perovskites. To form stable three-dimension (3D) structure, the selection of component ions can be predicted by the Goldschmidt tolerance factor, t.

$$t = \frac{R_X + R_A}{\sqrt{2}\left(R_X + R_B\right)}$$

R_A, R_B and R_X are the radius of A, B and X ions. It reveals the cubic perovskite formed if $0.9 \leq t \leq 1$. And hexagonal or tetragonal structure is with $t > 1$ and orthorhombic or rhombohedral structure is with $0.71 \leq t \leq 0.9$.[74, 75] In the early stage, the most common organic cations used in lead-based perovskites are the methylammonium ($CH_3NH_3^+$/MA). However, a bandgap of 1.55 eV ($MAPbI_3$) is not enough for panchromatic absorption due to the relatively short absorption limited to 800 nm. Indeed, the delicate tune of perovskite composition is found to have a large impact on the optoelectrical properties of the resultant perovskite materials. For instance, the replacement of MA with formamidinium (FA) was found to reduce the bandgap by about 0.07 eV, from 1.55 eV to 1.48V, giving rise to an extension of the absorption wavelength by about 40 nm.[76] The replacement of partial Pb^{2+} with Sn^{2+} leads the bandgap decreasing from 1.55 eV to 1.27 eV. [77] It is also observed that the change of halide can result in bandgap variation.[78] The direct impact from composition engineering is the change of perovskite properties, thus affecting the correspondent PVSC performance. In this section, we introduce the recent progresses of high performance PVSC achieved with the composition engineering of perovskites. And the content for perovskite stability derives from composition engineering will be discussed in the stability section.

The large size of FA cation (over that of MA) led to $FAPbI_3$ a high tolerance factor t >1, resulting a hexagonal yellow non-perovskite δ-phase at room temperature. It thus needs the careful investigation to improve the phase stability of black perovskite trigonal α-$FAPbI_3$ for practical solar cells. Jeon and Seok *et al.* investigated the performance of mixed perovskites, $(FAPbI_3)_{1-x}(MAPbBr_3)_x$ and demonstrated that incorporation of $MAPbBr_3$ into $FAPbI_3$ not only stabilizes the perovskite phase of $FAPbI_3$, but also improves the PVSC PCE beyond 18%.[41] Recently, Jacobsson and Hagfeldt *et al.* studied 49 different perovskite compositions which are obtained by independently varying the MA/FA and the I/Br-ratio in the mixed perovskites (**Figure 4a**).[40] It revealed that small changes in the perovskite composition have a large impact on the material properties (bandgap, energy level and morphology etc.) and the resultant device performance. For example, an increased amount of bromide increases the band gap, whereas an increased amount of FA decreases the band gap but to a smaller extent. While a larger amount of bromide in the perovskite was found to cause

intense sub band gap photoemission with detrimental results for the device performance. A sound explanation would be a phase separation with the formation of a minority phase with a lower band gap (i.e. iodide rich perovskite) and the majority phase. The photo-excited charge carriers could easily be trapped in this secondary minority phase, as illustrated in **Figure 4c–e**. As results, cell efficiencies improved from a few percent up to 20.7% with a composition of $FA_{4/6}MA_{2/6}PbBr_{0.5}I_{2.5}$.

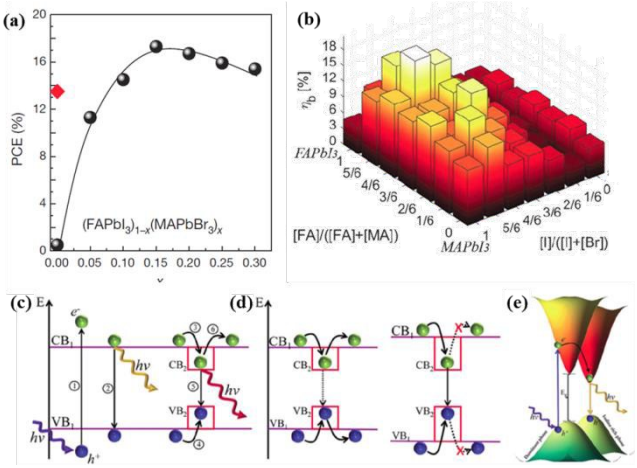

Figure 4. (a) and (b) PCE values for cells using different compositions of $(FAPbI_3)_{1-x}(MAPbBr_3)_x$;[40] (c) Illustration of trap assisted recombination with minority phase, and (d) the increase of band gap difference between the minority and the majority phase enhanced trapping probabilities. (e) Illustration of electron transfer from the majority to the minority phase. The cones are representative of the density of states at the conduction and valence band edges in the k-space of the perovskite. Adapted with permission from ref. [40] Copyright 2016 The Royal Society of Chemistry

Furthermore, inorganic cation, like cesium can be introduced to triple cation perovskite compositions (Cs/MA/FA), which produce new perovskites with improved thermal stability. Meanwhile, it gives purer α-$FAPbI_3$ phase that is less sensitive to processing conditions. The idea ratio of $Cs_{0.05}(MA_{0.17}FA_{0.83})_{0.95}Pb(I_{0.83}Br_{0.17})_3$ enables reproducible device performances to reach a stabilized power output of 21.1% and ~18% after 250 hours under operational conditions.[79] As shown in Table 1, we summarize the highest PCE reported for efficient perovskites with different composition. It is interesting to observe that a number of multi-compositional perovskites have device efficiencies near or over 20%, representing nowadays highly efficient PVSCs with mesoporous structure and/or planar structure.

As a brief conclusion, the material composition engineering is essential to generate a variety of perovskites with designed optoelectronic properties, some of which enable PVSCs with efficiencies over 20%. Further studies are needed to clarify the design rule of perovskite composition, since a complicate precursor composition would likely to make the film formation kinetics more difficult. Therefore, the desired composition should be the outcome of a fine balance among device efficiency, processing and stability etc. Apart from the high efficiency related to PVSCs, it has been previously showed that the J-V hysteresis behaviour also makes the determination of actual efficiency of PVSCs difficult. The efficiency obtained from reverse scan is usually inconsistent with forward scan, and higher scan rate would result in higher efficiency.[80-82] The origin of J-V hysteresis have been discussed, and ascribed to the reasons, such as ferroelectric polarization of perovskite[83], the trap states of the perovskite materials[84], ion migration[85], ionization-enhanced migration of hydrogen impurities etc. Although the definitive conclusion has not been pin-down yet, the recent progresses of PVSCs generally showed high performance with mitigated hysteresis.

Table 1 Summary of the highest PCE of perovskite solar cells with different compositions

PV Materials	Device structure	J_{SC} [mA cm^{-2}]	V_{OC} [V]	FF [%]	PCE [%]	Ref
$MAPbI_3$	ITO/PTAA/PV/C_{60}/BCP/Cu	24.0	1.11	78.0	20.7	86
$FAPbI_3$	FTO/bl-TiO_2/mp-TiO_2/PV/PTAA/Au	24.7	1.06	77.5	20.2	57
$MA_{0.6}FA_{0.4}PbI_3$	ITO/PTAA/PV/ICBA/C_{60}/BCP/Cu	23.0	1.03	77.0	18.3*	66
$Cs_{0.2}FA_{0.8}PbI_3$	FTO/SnO_2/C_{60}-SAM/PV/Spiro-OMeTAD/Au	22.2	1.09	80.8	19.6	87
$Cs_{0.15}FA_{0.85}Pb(I_{0.83}Br_{0.17})_3$	FTO/bl-TiO_2/mp-TiO_2/PV/Spiro-OMeTAD /Au	22.8	1.153	76.0	20.0	75
$FA_{0.81}MA_{0.15}PbI_{2.51}Br_{0.45}$	FTO/bl-TiO_2/mp-TiO_2/PV/Spiro-OMeTAD/Au	24.6	1.16	73.0	20.8	88
$Cs_{0.05}(MA_{0.17}FA_{0.83})_{0.95}Pb(I_{0.83}Br_{0.17})_3$	FTO/bl-TiO_2/mp-TiO_2/PV/PTAA/Au	23.5	1.15	78.5	21.1	89
$Rb_{0.05}[Cs_{0.05}(MA_{0.17}FA_{0.83})_{0.95}]_{0.95}Pb(I_{0.83}Br_{0.17})_3$	FTO/bl-TiO_2/mp-TiO_2/PV/Spiro-OMeTAD /Au	22.7	1.18	81.0	21.6	75

* doctor-blade coating

2.3 Interfacial Layers

In addition to the quality of perovskite absorbers, the electrical and electronic contact between photoactive layer and electrode is of critical to determine the performance of solar cells.[43-46, 90-94] Basically, It requires interfacial layer consisting hole transporting material (HTM) or electron transporting material (ETM) that selectively extract photo-generated charge from the perovskite film and transport to the corresponding electrode. To deal with organic-inorganic hybrid perovskite, recent studies also revealed interfacial materials can have additional effects, like passivation of trap states,[95] barrier for moisture,[96] and template for perovskite crystal growth[97] etc. Especially, hysteresis in PVSCs identified previously as mentioned above can also be healed with the proper interface

engineering. All these features are the available knobs that potentially boost up device performance and stability, as well as mitigate hysteresis. Essentially, it is important to develop novel interfacial materials for PVSCs.

Spiro-OMeTAD is a commonly used HTM in mesoporous PVSC and can give remarkable efficiency. Due to the low conductivity of pristine spiro-OMeTAD, they usually require additive doping for efficient hole extraction and transport, however, this results in complicated device processing and deteriorated device stability, which are major drawbacks for current PVSCs.[98, 99] Therefore, dopant-free and easily fabricated hole transport materials are necessary for PVSCs. [100, 101 102] Xu *et al*. developed an easily synthesized spiro-structured HTM X60 and got an efficiency of 19.84%,[103] which utilized low-cost spiro[fluorene-9,9'-xanthene] core to replace spirofluorene. Malinauskas *et al*. synthesized a new small-molecule HTM V826 based on OMeTAD-substituted fluorene fragments, obtaining an efficiency near 20%.[104] Saliba *et al*. designed HTM FDT with a simple dissymmetric fluorene–dithiophene core. The low-cost FDT based mesoporous PVSCs deliver an impressive efficiency as high as 20.2%.[105] Nishimura *et al*. developed Azulene 1 HTM by using a azulene core and four quasiplanar arylamines, giving a PCE of 16.5%.[106] Nevertheless, the above mentioned HTMs still need dopant to ensure outstanding performances in mesoporous devices.

Instead, the planar heterojunction device, i.e. p-i-n structure, which affords the use of thin and flat HTM layer underneath of the perovskite layer. So the stringent requirements on the HTM conductivity can be alleviated. Dopant-free HTMs have been designed for such structure, showing comparable efficiencies to those mesoporous devices. Among them, polymeric HTM, poly(3,4-ethylenedioxythiophene) polystyrene sulfonate (PEDOT:PSS) is widely used, but have adverse effects due to its hydroscopicity and acidity. To ensure the wetting ability to the perovskite precursor solution, Xue *et al*. synthesized a polymer HTM HSL2 with sodium sulfonate terminal group on the side chain, which is inserted between PEDOT:PSS and perovskite film, and a high PCE of 16.6% was achieved with negligible

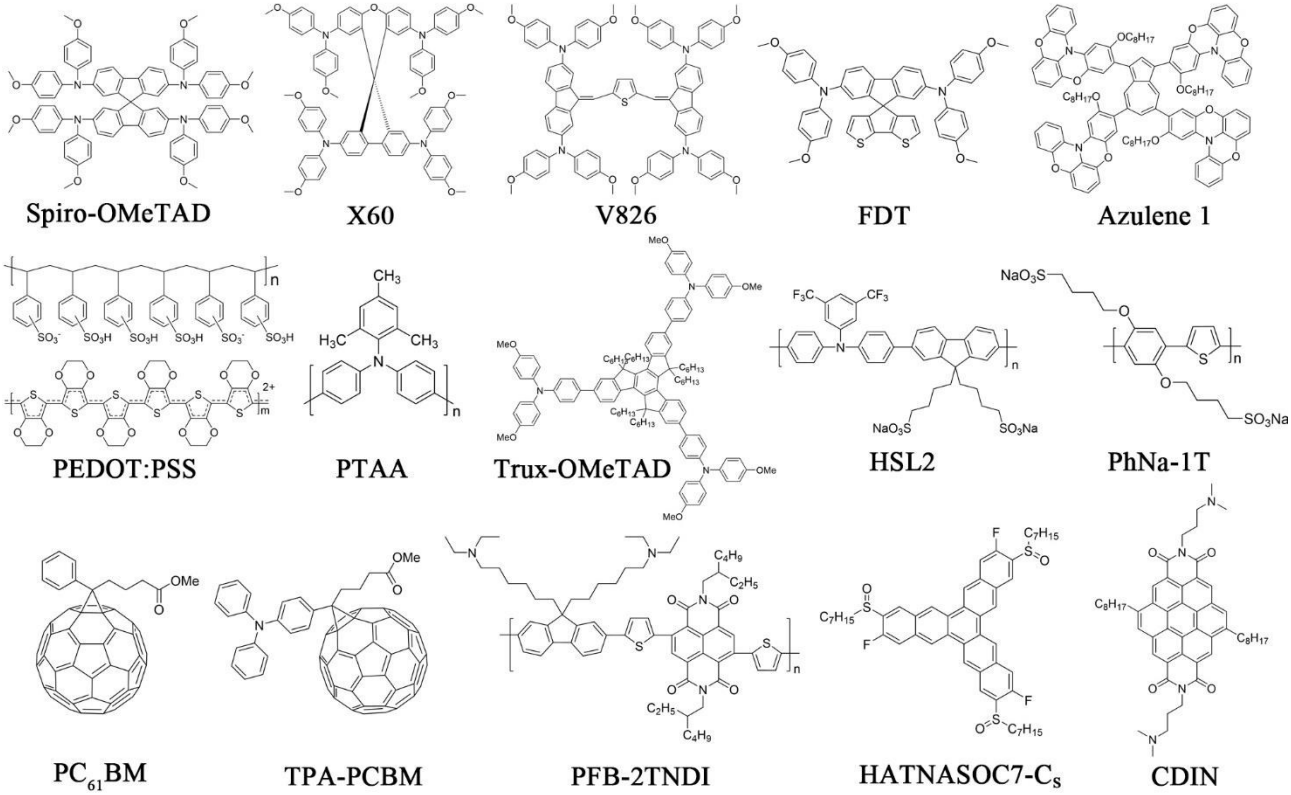

Figure 5 Molecular structures of efficient HTM and ETM (last row).

hysteresis.[107] Jo *et al*. also introduced the sodium sulfonate group to the side chain of polymer with a backbone of benzene and thiophene (PhNa-1T).[108] The flexible inverted device based on PhNa-1T exhibited a PCE of 14.7% with high hole-extraction and suppressed charge recombination.

Another classic polymeric HTM, poly(bis(4-phenyl)(2,4,6-trimethylphenyl)amine) (PTAA) and its analogues have been routinely used in planar devices. [109, 110] Bi *et al*. demonstrated that non-wetting HTM is beneficial to fabricated large perovskite grain size with the reduce of charge trap density, achieving an enhanced and stabilized efficiency of 18.1% from the PTAA based planar devices,[97] comparing with the device based on hydrophilic PEDOT:PSS. Small molecule HTMs are also promising for this application, whereas they are with good structure tunabilities. Huang *et al*. reported a truxene based dopant-free HTM Trux-OMeTAD. The planar and symmetrical truxene core promotes ordered molecular packing in solid, which facilitates a high hole mobility up to 10^{-3} cm^2 V^{-1} s^{-1} and enables an efficiency of 18.6% for the p-i-n planar PVSCs.[111]

Besides organic HTM, lots of interests have also been attracted to inorganic materials, especially nickel oxide.[112-114] Jung *et al*. reported a solution-processable Cu-doped NiO_x HTM for PVSC. Due to the enhanced crystallinity and conductivity brought by Cu, the resulting device shows an impressive PCE of 17.8%.[115] Zhang *et al*. demonstrated n-i-p planar PVSC employing solution-processed $CuGaO_2$ as HTM.[116] The dense $CuGaO_2$ layer with a high mobility can enhance the PCE to 18.51% and also improve the device long-term stability significantly by avoiding organic dopant. Yu *et al*. fabricated p-i-n planar PVSC based on a solution-processed CuO_x HTM which showed a PCE of 17.4% with good reproducibility and stability.[117]

As for the ETMs, metal oxides (like TiO_2 and SnO_2) as well as C_{60} fullerene and its derivatives (like phenyl-C_{61}-butyric acid methyl ester, $PC_{61}BM$), are commonly used for PVSCs. [91, 118-125] Desired ETM should exhibit suitable energetics and wide optical band gap, to maximize the photon absorption by perovskite layer and selectively extract electron while block hole at cathode side, to alleviate charge recombination at the device interface. Zhou *et al*. utilized yetrium-dopped TiO_2 (Y-TiO_2) as ETM to construct planar PVSC. A high PCE of 19.3% is achieved through the careful control of device interface and the formation of perovskite film.[126] Recently, SnO_2 has attracted interests as ETM due to its wide-bandgap, high transparency and high mobility.[127] Baena *et al*. demonstrated a 15 nm SnO_2 layer with mixed perovskite film to give a PCE of 18.4% with an outstanding high V_{OC} of 1.19 V.[128] Zuo *et al*. modified ZnO HTM in p-i-n devices with 3-aminopropanioc acid (C_3-SAM) to direct the crystalline process and improve the crystal quality.[129] The resulting devices could output an efficiency of 15.67%. However, the usual development of metal oxide, i.e. TiO_2 requires high temperature sintering and show performance degradation upon UV exposure. Regarding this, organic based ETM exhibits advantages such as mild solution-processing and good tunabilities etc.

New fullerene derivatives have been extensively studied. Regarding to the metal oxide defeats, a fullerene self-assembled monolayer can passivates the charge traps of metal oxide[130-132] and a fullerene unit towards perovskite reduces nonradiative recombination channels at the interface, which significantly improve photovoltaic performance with low hysteresis.[119, 133, 134] Fullerene derivatives, such as fullerene with ammonium salts,[96, 135-139] fullerene with folurolated chain,[124] or oligoether side group chain,[140, 141] or crown-ether[142], or cyanoacetate moieties[100] is developed to facilitate the fabrication of stable and efficient PVSCs. It was previously revealed that the in-situ anion-induced electron transfer (AIET) between certain anions of ammonium salts and fullerene, as well as other n-type materials facilitate the intrinsic n-type doping to improve charge transport and work function tunabilities of organic ETM layers.[143-146] Li *et al*. demonstrated that intramolecular charge transfer characteristics of triphenylamine functionalized fullerene TPA-PCBM could improve molecular polarization, carrier density and charge transport capability, leading to 13% enhancement in J_{SC} compared with $PC_{61}BM$.[147]

In the meantime, non-fullerene organic ETMs have merits of good structural tunabilities with low cost, but remain less explored.[148-151] Sun *et al*. reported a polymer ETM PFN-2TNDI containing naphthalene diimide and amine end-capped side chain.[149] It can achieve a high PCE of 16.7% for PVSC, since ETM itself is conductive, while adjusting the electrode work function and passivating perovskite surface defects. Zhao *et al*. developed a small molecule, HATNASOC7-C_S and used it as ETM to construct p-i-n devices, which showed a superior PCE of 17.6%.[150] Recently, a discotic coronene diimide (CDI) core based ETM, CDIN is developed. The large, extended π-conjugated CDI plane is favourable for strong π-π stacking to enhance charge mobility, resulting in a high efficiency over 17% in n-i-p devices.[151]

As a brief conclusion, a good number of interfacial materials are developed with a variety of functionalities, which largely enriched both the planner and mesoporous PVSCs to over 18% PCE, up to 22.1% PCE to date. For the perspectives, some controlling features would be desired for further exploration of new HTM and ETM, such as the capabilities to guide perovskite crystal growth, to passivate the defeats, and to protect perovskite from moisture and Uv-light degradation, in addition to the conventional considerations on charge mobility, energy level and work-function tunabilities of interfacial layers.

2.4 Tandem Solar Cells

In addition to the extensive studies in single junction PVSCs, the exploration of multiple junction devices, like tandem and parallel solar cells[152-155] is believed to be an effective strategy for reaching higher efficiencies and overcome the Shockley-Queisser limit in single junction devices. In tandem devices, high and low energy photons can be selectively harvested by the front and rear cells with different bandgaps, which electrically collected through a transparent internal electrode.[152-154] Due to the tunable bandgaps between 1.17 and 2.3 eV,[156, 157] low-cost perovskites are particularly attractive in constructing tandem devices by themselves, or interfacing with a variety of solar cells, such as silicon, copper indium gallium selenide (CIGS) and OSCs. Theoretical prediction suggests that the peak efficiency for the mechanically stacked tandem is 37.2% and 35.7% for monolithic tandem when combing a 1.6 eV perovskite solar cell and a Si solar cell with theoretical peak efficiency (29.4%).[158, 159]

The perovskite containing tandem solar cells are mainly fabricated in two types of configuration: mechanically stacked 4-terminal tandems and monolithic 2-terminal tandems. The structures are shown in **Figure 6**. In 4-termianl tandems, the two cells are fabricated independently and mechanically stacked on top of each other, while the monolithic tandems electrically connect two subcells through a transparent internal electrode. The presence of an extra transparent electrode in 4-terminal devices results in additional absorption losses and device cost. The challenges associated with the 2-terminal perovskite tandem solar cells include the development of charge recombination layer and the complicated multi-layer fabrication, as well as the delicate optimization of sub-cell thickness to ensure the current match in between. Table 2 presents the current status of various types of perovskite tandem devices reported in the literatures.

Silicon is the most widely investigated small-bandgap materials as rear cells for perovskite tandems. McMeekin and Snaith *et al.* combined $Cs_{0.17}FA_{0.83}Pb(I_{0.6}Br_{0.4})_3$ with an optimized optical band gap of 1.75 eV with a 19%-efficiency silicon cell and demonstrated the feasibility of achieving >25% PCE 4-terminal tandem solar cells.[160] The small-bandgap materials can also be perovskites. Yang and Jen *et al.* developed $MA_{0.5}FA_{0.5}Pb_{0.75}Sn_{0.25}I_3$ with a low bandgap of 1.33 eV as rear cell, and when it was combined with $MAPbI_3$ as front cell, 4-terminal tandem device with efficiency up to 19.08% can be achieved.[161] Eperon and Snaith *et al.* developed an infrared absorbing 1.2 eV bandgap perovskite, $Cs_{0.25}FA_{0.75}Pb_{0.5}Sn_{0.5}I_3$, as rear cell. By combining with a wider bandgap $Cs_{0.17}FA_{0.83}Pb(I_{0.5}Br_{0.5})_3$ with a bandgap of 1.6 eV, they reached monolithic 2-terminal tandem efficiencies of 17.0% and obtained 4-terminal tandem cells with 20.3% efficiency.[39]

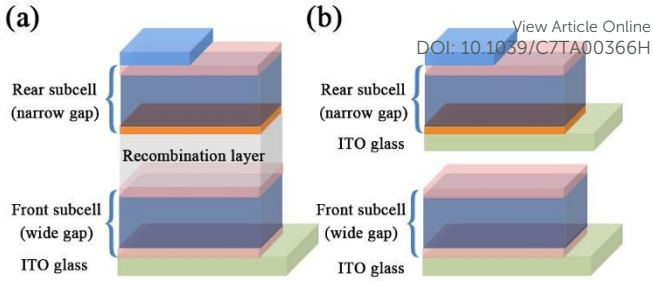

Figure 6. Schematics showing (a) 2-terminal (2T) and (b) 4-terminal (4T) tandem perovskite solar cells.

As above, perovskite-based tandem solar cells are mainly the combination of wide bandgap PVSCs with other highly efficient small bandgap solar cells, like silicon or CIGS. Since the bandgap of perovskite materials can be easily tuned, fully perovskite tandem solar cells are also developed. Low bandgap perovskites include the unstable Sn^{2+}, temporally show adverse influence on the device long-term stability. Therefore, at current stage, the combination of wide bandgap and efficient PVSCs with other state-of-the-art low bandgap silicon or CIGS solar cells may be a bright choice for further development.

Table 2 Summary of high efficiency perovskite-based tandem solar cells.

Type	Front Cell	Bandgap/eV	Rear Cell	Bandgap /eV	PCE/%	Year	Ref
4-terminal	$MAPbI_3$	1.55	mc-Si	1.1	17.0	2014	162
4-terminal	$MAPbI_3$	1.55	c-Si	1.1	13.4	2015	163
4-terminal	$MAPbI_3$	1.55	c-Si	1.1	18.0	2015	164
2-terminal	$MAPbI_3$	1.55	c-Si	1.1	18.0	2015	165
2-terminal	$MAPbI_3$	1.55	c-Si	1.1	21.4	2015	166
4-terminal	$MAPbI_3$	1.55	c-Si	1.1	23.0	2016	167
4-terminal	$MAPbI_3$	1.55	c-Si	1.1	25.2	2016	168
2-terminal	$MAPbI_3$	1.55	c-Si	1.1	20.6	2016	168
4-terminal	$Cs_{0.17}FA_{0.83}Pb(I_{0.6}Br_{0.4})_3$	1.74	c-Si	1.1	25.2	2015	160
2-terminal	$MAPbI_3$	1.55	$Cu_2ZnSn(S,Se)_4$	1.1	4.6	2014	169
4-terminal	$MAPbI_3$	1.55	CIGS	1.1	18.6	2014	162
2-terminal	$MAPbI_3$	1.55	CIGS	1.04	10.9	2015	170
4-terminal	$MAPbI_3$	1.55	CIGS	1.08	20.5	2015	171
2-terminal	$MAPbI_3$	1.55	PBSeDTEG8	1.28	10.23	2015	172
2-terminal	$MAPbBr_3$	2.25	$MAPbI_3$	1.55	10.8	2015	157
4-terminal	$MAPbI_3$	1.55	$MA_{0.5}FA_{0.5}Pb_{0.75}Sn_{0.25}I_3$	1.33	19.08	2016	161
2-terminal	$Cs_{0.15}FA_{0.85}Pb(I_{0.3}Br_{0.7})_3$	2	$MAPbI_3$	1.55	18.1	2016	173
2-terminal	$Cs_{0.17}FA_{0.83}Pb(I_{0.5}Br_{0.5})_3$	1.8	$Cs_{0.25}FA_{0.75}Pb_{0.5}Sn_{0.5}I_3$	1.2	17.0	2016	174
4-terminal	$Cs_{0.17}FA_{0.83}Pb(I_{0.5}Br_{0.5})_3$	1.8	$Cs_{0.25}FA_{0.75}Pb_{0.5}Sn_{0.5}I_3$	1.2	20.3	2016	174

3. Perovskite Materials and Device Stability

The efficiency for common $MAPbI_3$ and $FAPbI_3$ based PVSCs is fairly high. However, the long-term operational stability is still a big challenge for PVSCs. The origin of the instability of devices can be mainly ascribed to unstable perovskite materials, which tends to decompose under environmental stresses, such as humidity, heat and prolong light illumination in air. The possible decomposition mechanism of $MAPbI_3$ under humidity and light is suggested as following equation 1 to 6. $MAPbI_3$ first decompose into solid PbI_2 and CH_3NH_3I. Then CH_3NH_3I further decompose into aqueous CH_3NH_2 and HI.[36] Likewise, HI could convert into iodine upon oxidation or photon excitation (Eq. 1-4). $MAPbI_3$ also decomposes into CH_3NH_2 gas and HI gas under light illumination (Eq. 5-8).[36]

View Article Online
DOI: 10.1039/C7TA00366H

$$CH_3NH_3PbI_3 \xrightleftharpoons{H_2O} PbI_2 + CH_3NH_3I(aq.) \quad (1)$$

$$CH_3NH_3I(aq.) \rightleftharpoons CH_3NH_2(aq.) + HI(aq.) \quad (2)$$

$$4\ HI(aq.) + O_2 \rightleftharpoons 2\ I_2 + 2\ H_2O \quad (3)$$

$$2\ HI(aq.) \xrightleftharpoons{hv} H_2\uparrow + I_2 \quad (4)$$

$$CH_3NH_3PbI_3 \xrightleftharpoons{hv} PbI_2 + CH_3NH_2\uparrow + HI\uparrow \quad (5)$$

$$2\ I^- \xrightleftharpoons{hv} I_2 + 2\ e^- \quad (6)$$

$$3\ CH_3NH_3^+ \xrightleftharpoons{hv} 3\ CH_3NH_2\uparrow + 3\ H^+ \quad (7)$$

$$I^- + I_2 + 3\ H^+ + 2\ e^- \rightleftharpoons 3\ HI\uparrow \quad (8)$$

To improve the stability of PVSCs, both stable perovskite materials and devices should be put under consideration. Still, the composition engineering is effective to obtain intrinsically stable perovskite with good properties. For the device stability, proper protection means are also necessary to ensure the robustness of PVSCs. In this section, we introduce approaches developed so far to address the stability issue of PVSCs, including two aspects, material and device.

3.1 Stable Perovskite Materials

The prototypical $MAPbI_3$ is known to suffer a phase transition from cubic to tetragonal at about 55 ℃, which has adverse effect for its performance.[175, 176] To improve the thermal stability of perovskite, strategies involving the usage of polymer, i.e. polyvinylpyrrolidone (PVP) to stabilize the cubic $MAPbI_3$ perovskite,[177] which, however, cannot solve the problem totally. Besides, $MAPbI_3$ is easy to decompose into PbI_2 under humidity, heat, light and oxygen.[36, 178-186] Intriguingly, It is revealed that $MAPbI_3$ may form a hydrate intermediate $MAPbI_3{\cdot}H_2O$ before further decomposing into PbI_2.[183] Some DFT results suggest that the water absorption of $MAPbI_3$ is dramatically influenced by the orientation of MA cations near the surface.[187] For a stable PVSC, high quality perovskite film is a primary requirement. Some additives are reported to improve the efficiency and stability of PVSCs simultaneously by improving the perovskite film quality, such as chloride ion and PCBM.[188, 189]

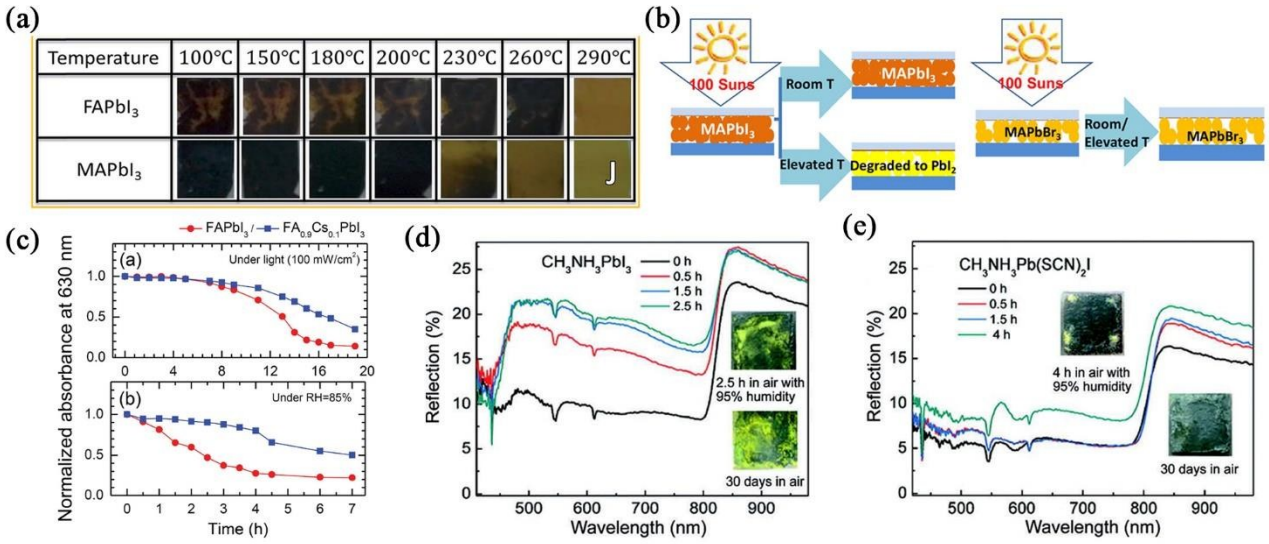

Figure 7 The Comparison of Perovskite Material Stabilities: (a) images of $FAPbI_3$ and $MAPbI_3$ after annealing.[190] (b) $MAPbI_3$ and $MAPbBr_3$.[179] (c) Normalized absorbance of $FAPbI_3$ and $FA_{0.9}Cs_{0.1}PbI_3$ films.[191] Reflection spectra of (d) $MAPbI_3$ and (e) $MAPb(SCN)_2I$.[192] Adapted with permission from ref. [190] and [192] Copyright 2015 The Royal Society of Chemistry, from ref. [179] Copyright 2015 American Chemical Society, from ref. [192] Copyright 2015 Wiley-VCH Verlag GmbH & Co. KGaA.

To play with cations, $FAPbI_3$, is more thermally stable than $MAPbI_3$ (**Figure 7a**), but undergoes a phase transition from black perovskite trigonal α-$FAPbI_3$ to yellow hexagonal δ-$FAPbI_3$ phase in the presence of moisture, due to a large tolerant factor from FA.[76, 190, 193] Fortunately, it turns out the compositional engineering is effective and promising to tackle this problem. MA-FA mixed perovskite shows higher structural stability than pure FA perovskite.[194, 195] Concerned about the instability of organic cation, fully inorganic perovskite $CsPbBr_xI_{3-x}$ is explored with good stability (**Figure 7b**).[179, 196-199] Swarnkar *et al.* successfully fabricate phase-stable α-$CsPbI_3$ quantum dots solar cells in ambient air and achieve a high efficiency of 10.77%,[200] though the α-$CsPbI_3$ is reported only stable at high temperature. Moreover, partial substitution of FA with inorganic cation Cs in FA-based perovskites is also demonstrated to improve the photo and thermal stability of perovskite materials, which is ascribed to the enhanced interaction between FA^+ and I^- as a result of the contraction of cubo-octahedral volume (**Figure 7c**).[191]

As indicated in the decomposition routes, the instability of $MAPbI_3$ perovskite involves the release of side-product HI due to the decomposition of MAI. Some works showed that replacing part of iodide with bromide in perovskites allows improving material stability and tuning the bandgaps of

perovskites. [76, 151, 201, 202] Combining the advantages of FA cation and bromide anion, Jeon and Seok *et al.* first reported the multi-compositional $(FAPbI_3)_{0.85}(MAPbBr_3)_{0.15}$ perovskite, exhibiting both good efficiency and structural stability.[41] It becomes a prototype of high efficiency perovskite materials.[88, 192, 203] Later, inorganic cations are also incorporated into multiple cation perovskites, such as $Cs_{0.05}(MA_{0.17}FA_{0.83})_{0.95}Pb(I_{0.83}Br_{0.17})_3$[89] and $Rb_{0.05}[Cs_{0.05}(MA_{0.17}FA_{0.83})_{0.95}]_{0.95}Pb(I_{0.83}Br_{0.17})_3$,[75] to improve material and device stability.

The use of pseudohalogen to partially replace halide is also explored. Jiang *et al.* first introduced thiocyanate anion (SCN^-), which have similar radius to iodide, to partially substitute iodide in $MAPbI_3$. The resulted perovskite $MAPb(SCN)_2I$ shows comparable efficiency to $MAPbI_3$ but higher moisture stability due to stronger interaction between SCN^- and Pb^{2+}.[204] (**Figure 7d-e**) Others suggested that 2D layered perovskite $MA_2Pb(SCN)_2I_2$ would be formed instead of 3D structure, and it is thermodynamically stable.[205-207] Umeyama *et al.* indicated that $MA_2Pb(SCN)_2I_2$ is likely to decompose into $MAPbI_3$ under high humidity or annealing condition, in which case it is more like an intermediate.[208] Thiocyanate additive is also found to promote the formation of α-$FAPbI_3$.[92]

Recently, the development of two-dimension (2D) perovskites also exhibits good tendency to improve material stability. For instance, the usage of large ammonium cation with hydrophobic group favours the formation of stable 2D perovskite, but sacrificing efficiency. Smith *et al.* first introduced $C_6H_5(CH_2)_2NH_3^+$ (PEA) to make a layered perovskite $(PEA)_2(MA)_2[Pb_3I_{10}]$[209], which is stable under moisture due to

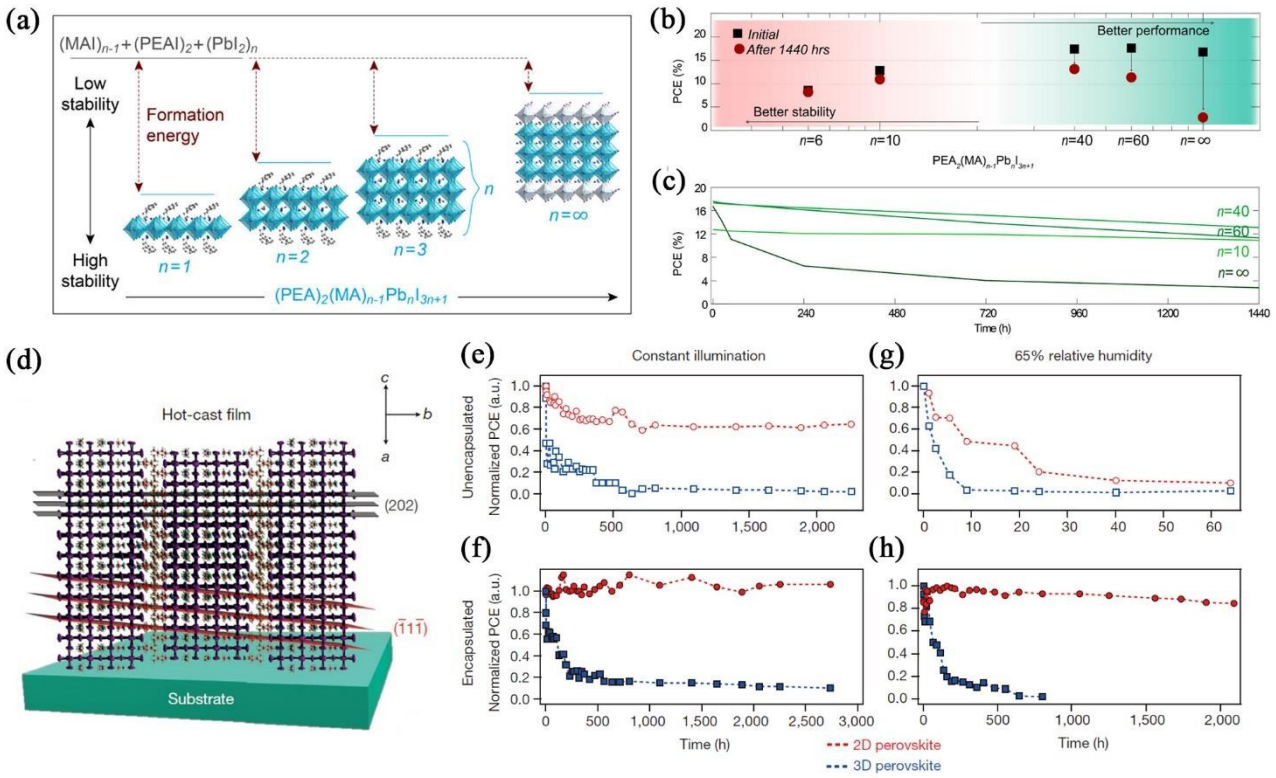

Figure 8 (a) Unit cell structure of $(PEA)_2(MA)_{n-1}Pb_nI_{3n+1}$ perovskites. (b) Device performance and (c) performance evolution of $(PEA)_2(MA)_{n-1}Pb_nI_{3n+1}$ based PVSCs (stored in nitrogen).[210] (d) Schematic representation of the (101) orientation, along with the (111) and (202) planes of a 2D $(BA)_2(MA)_3Pb_4I_{13}$ perovskite crystal. Photostability and Humidity stability tests PVSCs without (e and g) and with (f and h) encapsulation. 2D perovskite: $(BA)_2(MA)_3Pb_4I_{13}$, red; 3D perovskite: $MAPbI_3$, blue.[211] Adapted with permission from ref. [210] Copyright 2016 American Chemical Society, from ref. [211] Copyright 2016 Nature Publishing Group.

View Article Online
DOI: 10.1039/C7TA00366H

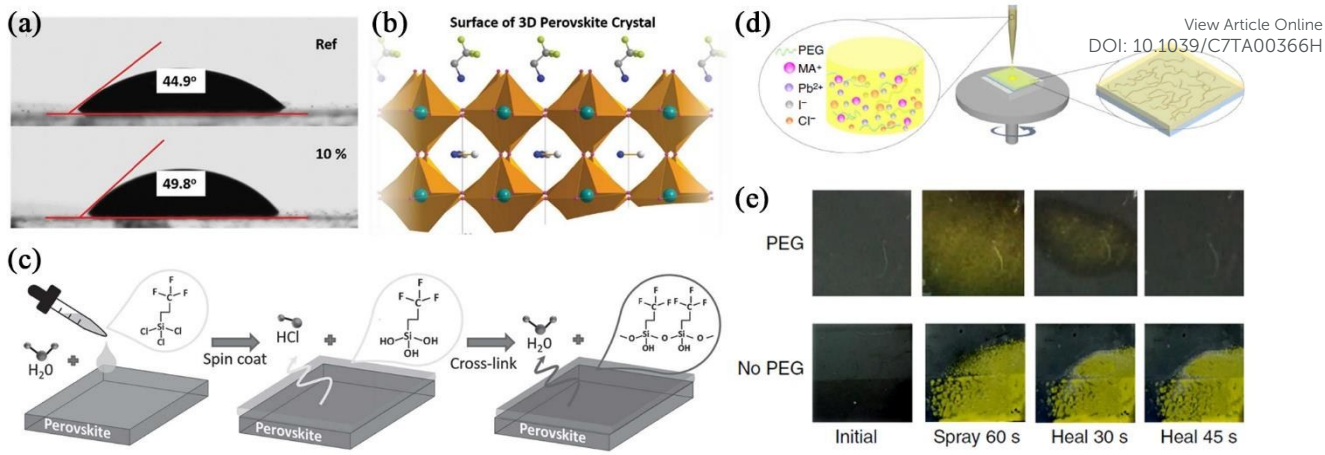

Figure 9 (a) The static contact angles of the perovskite films without and with 10% FEAI with deionized water. (b) Schematic model of FEAI modified $MAPbI_3$.[212] (c) Cross-link process of fluoro-silane layer on the perovskite film.[213] (d) Fabrication process of perovskite film with PEG scaffold. (e) Water-spraying test of perovskite films with and without PEG.[214] Adapted with permission from ref. [212] and [213] Copyright 2016 Wiley-VCH Verlag GmbH & Co. KGaA, from ref. [214] Copyright 2016 Nature Publishing Group.

the hydrophobic nature of benzene group. However, the efficiency (4.73%) for layered perovskites is much lower compared to 3D PVSCs (over 20%).

Combination of large ammonium cations, like PEA and $CH_3(CH_2)_3NH_3^+$ (BA) with common MA are later found to form mixed-dimensional (quasi-2D) perovskite $(RA)_2(MA)_{n-1}Pb_nI_{3n+1}$ (RA: PEA or BA), which exhibits improved stability (**Figure 8a**). Moreover, the number of inorganic lead iodide sub-layers (n in the chemical formula) in each layer can be easily tuned by simply adjusting the perovskite precursor, as well as their bandgaps. [215, 216] DFT results imply that the larger n corresponds to lower formation energy, but easier to decompose into precursor (**Figure 8b-c**).[210] Tsai *et al.* developed a 2D Ruddlesden-Popper perovskite $(BA)_2(MA)_3Pb_4I_{13}$ with near-single-crystalline quality, whose preferential growth orientation is perpendicular to the substrate, facilitating the charge transport and therefore dramatically improving the efficiency to 12.52% and retaining high photo and humid stability (**Figure 8d-h**).[211]

Recent strategies, such as multi-compositional perovskite and 2D perovskite shed light in achieving stable materials and devices. Through encouraging, it can be envisioned that the tremendous efforts are still needed to generate intrinsically stable perovskites with possibilities to extend the lifespan of PVSCs into decades.

3.2 Device Operational Stability

In addition to the material stabilities, the long device lifetime of PVSCs is the ultimate goal. It requires proper means to prevent the water, air and high energy photons into device destroying perovskite, and to prevent the degradation of electrode, thus improving the device stability. Firstly, the application of barrier layers directly onto perovskite and devices has been employed, showing positive effect in improving device stability under environmental stresses. Yang *et al.* introduced hydrophobic ammonium ions as water-resisting layer to modify the perovskite surface to improve the humid stability of perovskite materials.[217] Bi *et al.* incorporated an amphiphilic 1,1,1-trifluoro-ethyl ammonium iodide (FEAI) to modify the perovskite surface, which functions as moisture-resistant layer due to the hydrophobic CF_3 groups.[212] (**Figure 9a-b**) Zhao *et al.* utilized PEG, a water absorption polymer to prevent water from penetrating into perovskite, and also to retain the MAI, which shows a self-healing behaviour of perovskite when the retained MAI reacts with PbI_2 again.[214] (**Figure 9d-e**) Wang *et al.* used hydrophobic fluoro-silane layer to protect the underneath perovskite film, making the perovskite film much more stable in water (**Figure 9c**).[213]

Interestingly, Bella *et al.* coated a hydrophobic fluoropolymer as barrier layer on both the front side and back side of the device to block the permeation of water.[218] With the further assistance of luminescent downshifting fluorescent dye into front barrier layer, the studied PVSCs have showed the improvement of efficiency and light stability, due to fluorescent dye harvest ultraviolet light re-emit into the visible range, while fluoropolymer barrier blocks water and air. The PVSCs exhibit high efficiency near 19% and high stability, which retains 98% of its original efficiency after 6 months of photo and environmental stresses aging test (**Figure 10**).

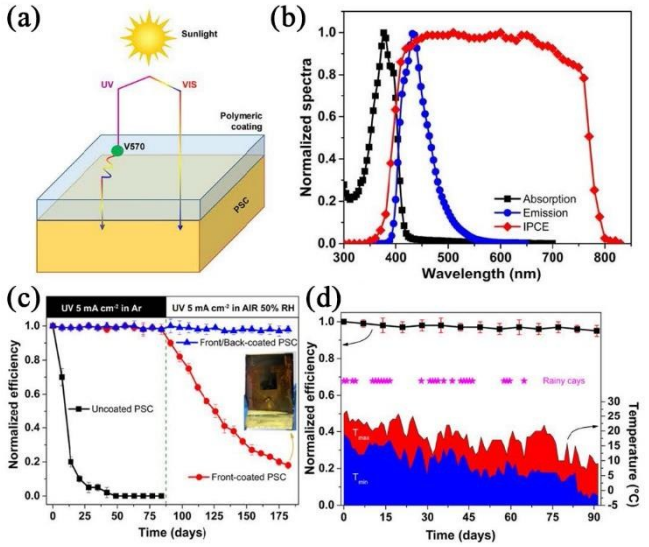

Figure 10 (a) Schematic illustration of the operational principle for the fluoropolymer barrier layer with fluorescent dye. (b) Normalized absorption and emission of dye-doped barrier layer compared to the PVSC IPCE. (c) Aging test on the three series of PVSCs: uncoated, front-coated and front/back coated. (d) Aging test on front/back coated devices on the terrace of the Italy.[218] Adapted with permission from ref. [218] Copyright 2016 American Association for the Advancement of Science.

Secondly, it is recently revealed that the erosion of metal electrode (Ag, Au and Al) upon the reaction with I and/or I_2 facilitates the degradation of PVSCs. To address this issue, stable electrodes are introduced. Deng *et al.* demonstrated that Cu electrode is stable in efficient PVSCs (**Figure 11a-c**).[66, 86] Domanski *et al.* intercalated a metal Cr interlayer between HTL and gold electrode to block the migration of gold into perovskite films, obtaining stable solar cells.[219] Back *et al.* introduced an amine-mediated metal oxide interlayer between $PC_{61}BM$ and silver to prevent the migration of iodide to the electrode, therefore stabilizing the silver electrode.[220] Interestingly, Mei *et al.* reported a fully printable PVSC with carbon electrode (**Figure 11d**).[221] It is reported that the carbon electrode not only effectively block humidity in ambient, but also remain its own stability, eventually leading to stable devices.(**Figure 11f**) Fully printable PVSC modules were also fabricated,[222] which performed well outdoor (**Figure 11e**).[223]

In this section, we survey recent researches related to device stabilities. Some approaches such as blocking layers atop of perovskite, proper device encapsulation and the choice of electrodes, have been developed, in which the principle is to essentially prevent perovskite from the exposure of environmental moisture and Uv-light.

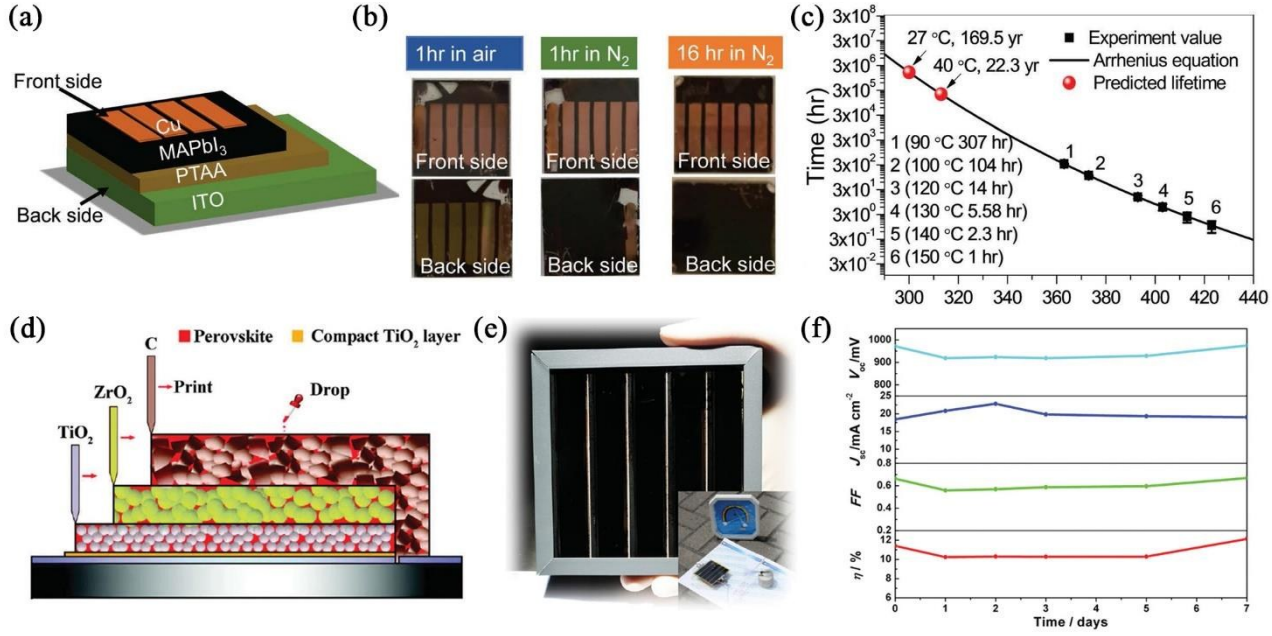

Figure 11 (a) Device structure for stability evaluation and (b) Photos of devices with different electrodes after being annealed at 100 ℃. (c) Measured perovskite material stable time at different temperature.[86] (d) Schematic of fully printable PVSC with carbon electrode.[221] (e) Image of a large-area (10 cm × 10 cm) fully printable PVSC module.[222] (f) Outdoor aging of the encapsulated PVSC in Jeddah, Saudi Arabia.[223] Adapted with permission from ref. [86] Copyright 2016 The Royal Society of Chemistry, from ref. [221] Copyright 2014 American Association for the Advancement of Science, from ref. [223] Copyright 2015 Wiley-VCH Verlag GmbH & Co. KGaA.

4. Lead-free Perovskite Solar Cells

It is known that the soluble lead salts in perovskite are toxic upon the exposure to human, and the release in environment causes pollution.[224-226] Although lead is currently allowed in photovoltaic modules, it should be desirable to find alternatives to replace lead halide perovskites for the long run.[227] Hence, the research of lead-free perovskite is motived. Theoretical studies suggest that cation Pb^{2+} plays a significant role in determining electronic structure of Pb-based perovskites, which participates in forming the conduction band minimum (CBM) and valence band maximum (VBM) of perovskites, especially the lone pair electrons $6s^2$ in Pb^{2+} ion.[228, 229] And the role of organic cation in $MAPbI_3$ is to stabilize the perovskite structure and change the lattice constant.[230, 231]

Therefore, it remains big challenges to find a perfect replacement to Pb^{2+} ion without scarifying the performance of PVSCs. Lots of efforts have been made to screen other common nontoxic divalent metal cations and those cations with lone pair electrons in the outer s orbitals like Bi^{3+}. Another solution is developing new derivatives with potential competence to Pb-based perovskites. In this section, we will review the recent progress of lead-free perovskites.

4.1 Tin-based Perovskite

Sn is the extensively explored substituent to Pb because it is in the same periodic group and has outer lone pair electrons. The Pb in $MAPbI_3$ can be fully replaced by Sn to form $MASnI_3$. However, Sn^{2+} has a poor chemical stability and would be easily oxidized to Sn^{4+}. Compared to $MAPbI_3$, $MASnI_3$ have a broader absorption to 950 nm,[232] corresponding to a narrower bandgap. Noel *et al*. achieved the highest efficiency of 6.4% for a $MASnI_3$ based mesoporous PVSCs, [233] which is behind of Pb-based PVSCs.[234, 235] Since the instability of Sn, Sn-based PVSCs usually have poor performance and reproducibility. In order to alleviate the oxidization of $MASnI_3$, Hoshi *et al*. introduced $HOOC(CH_2)_4NH_3I$ (5-AVAI) into the $MASnI_3$ to alleviate the oxidization of Sn^{2+} to improve the device stability. [236] Koh *et al*. incorporated SnF_2 into $FASnI_3$ to improve the film morphology as well as retarding the oxidization of Sn^{2+}.[237] SnF_2 additive can also reduce the defect concentrations in $CsSnI_3$ for a high photocurrent.[238] Lee *et al*. used SnF_2-pyrazine complex to further improve the morphology of $FASnI_3$. Consequently, they achieved an efficiency of 4.8% and the capsulated device also shows improved stability.[239]

Sn-based perovskite can be easily tuned by adjusting the perovskite composition. For instance, the bandgap of $MASnBr_xI_{3-x}$ gradually increases as the content of bromide increases. It is also found no obvious correlation between the ion radius and bandgap for $ASnI_3$ (A: Cs, MA, FA), while the bandgap of $APbI_3$ would decreases as the radius of A increases. [240] Although inorganic $CsSnI_3$ is reported to be more stable, its efficiency is only 3.56% and the chemical instability Sn^{2+} is still here, which put obstacle for real application. [232 241, 242] The Cs_2SnX_6 perovskite (X: I, Br, Cl) is also scrutinized, which has discrete $[SnI_6]^{2-}$ octahedral with Sn^{4+} centre while half of tin ion in $MASnI_3$ are missing (**Figure 12a**). Cs_2SnX_6 has a direct bandgap of ~1.3 eV and it is much more stable than $MASnI_3$ because Sn^{4+} is chemically stable. Nevertheless, it is an n-type semiconductor, which may be more suitable as ETM for solar cells.[243]

Since the pure Sn-based perovskites is instable, the mixed Sn-Pb perovskite would be a better choice. Zuo *et al*. reported the mixed $MASn_{1-x}Pb_xI_3$ PVSCs and achieved a highest efficiency of 10.1% when the content of Sn is 15%.[244] Notably, the bandgap of $MASn_{1-x}Pb_xI_3$ perovskite is narrower than both pristine $MASnI_3$ and $MAPbI_3$ perovskites (**Figure 12b**).[156] The TD-DFT calculation indicates that the bandgap of $MASn_{1-x}Pb_xI_3$ would decrease as x ($x < 0.5$) increases because of the stronger spin-orbit coupling of Pb, while the bandgap of $MASn_{1-x}Pb_xI_3$ would increase as x ($x > 0.5$) increases owing to the phase transition from *P4mm* to *I4cm* at $x > 0.5$. This opposite trends makes $MASn_{1-x}Pb_xI_3$ perovskite have an abnormal bandgap behaviour.[245] Moreover, Im *et al*. also found that the electronic structures of $MASn_{1-x}Pb_xI_3$ would be more similar to $MASnI_3$ rather than $MAPbI_3$ in case x is larger than 0.875.[245]

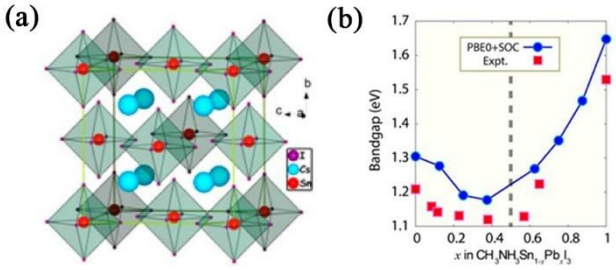

Figure 12 (a) Structure of Cs_2SnI_6.[243] (b) Experimental and calculated band gap evolution of $MASn_{1-x}Pb_xI_3$ solid solution as a function of composition x.[245] Adapted with permission from ref. [243] Copyright 2014 American Chemical Society, ref. [245] Copyright 2015 American Chemical Society.

4.2 Bismuth-based Perovskite

Recently, Bi-based perovskites have also drawn great attention, whose chemical formula is $A_3Bi_3I_9$ (A: MA, Cs).[246-250] It forms discrete two face-sharing octahedra $Bi_3I_9^{3-}$ and the cation A^+ occupies the space between them, which is actually a zero-dimension (0D) perovskite (**Figure 13a-b**). Hoye *et al*. demonstrated that $MA_3Bi_3I_9$ (MBI) is more stable than $MAPbI_3$ (**Figure 13c**).[251] In contrast to that $MAPbI_3$, MBI did not degrade to BiI_3 in humid air by forming a surface layer that does not increase the recombination rate. Park *et al*. first reported the application of Bi-based perovskite materials in solar cells and obtained efficiencies of 0.12% and 1.09% for MBI and $Cs_3Bi_3I_9$ respectively.[252] Zhang *et al*. fabricated MBI on the ITO/planar TiO_2/mesoporous TiO_2 substrate and achieved an efficiency of 0.42%.[253] All the Bi-based PVSCs have a small J_{sc}, which may be ascribed to the lack of continuous structural network. Other Bi-based perovskites $A_3Bi_3I_9$ (A: K, Rh, NH_4^+) are investigated as well, which, unlike MBI, have a 2D structure.[248, 249] However, no application in PVSCs for these 2D materials is reported yet.

View Article Online
DOI: 10.1039/C7TA00376H

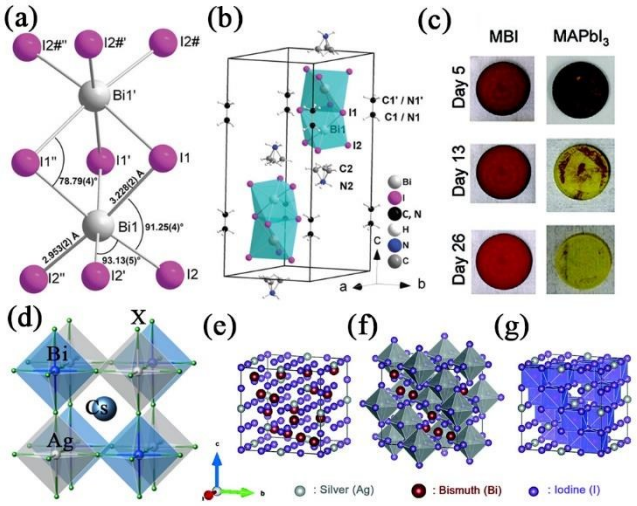

Figure 13 (a) Structure of the $Bi_2I_9^{3-}$ anion. (b) Cation and anion positions in the unit cell of $MA_2Bi_2I_9$.[247] (c) Photographs of MBI and MAPbI3 on quartz over time in ambient air.[251] (d) Structure of $Cs_2AgBi(Cl,Br)_6$.[254] (e) Representative $AgBi_2I_7$ cubic structure. The unit cell of $AgBi_2I_7$ is expressed with (f) six-coordinated silver-iodide octahedron sites and (g) eight-coordinated bismuth-iodide hexahedron sites.[255] Adapted with permission from ref. [247] Copyright 2016 The Royal Society of Chemistry, from ref. [254] Copyright 2016 American Chemical Society, from ref. [251] and [255] Copyright 2016 Wiley-VCH Verlag GmbH & Co. KGaA.

Another derivatives, such as halide double perovskites Cs_2AgBiX_6 (X: Br, Cl)[254, 256, 257] and $(MA)_2KBiCl_6$[258] are also developed, whose structure is similar to elpasolites (**Fig. 14d**). Both $Cs_2AgBiBr_6$ and $Cs_2AgBiCl_6$ are indirect bandgap semiconductors and their bandgaps are 2.19 eV and 2.77 eV, respectively.[254] $(MA)_2KBiCl_6$, however, have a large bandgap of 3.04 eV, which cannot be applied in solar cells. Some DFT calculation implied that $(MA)_2TlBiI_6$ is a potential lead-free perovskite material due to its similar property to $MAPbI_3$.[259] However, Tl is also very toxic, which is against the original intention for substituting lead. Kim *et al*. reported bimetal iodide $AgBi_2I_7$,[255] whose structure is a combination of AgI_6 octahedra and BiI_8 hexahedra (**Fig. 14e-g**). This material can form film with good morphology and its highest efficiency is 1.22%. Besides, it shows an excellent stability under ambient environment. Fabian *et al*. recently reported another bismuth iodide based perovskite $HDABiI_5$ (HDA: 1,6-hexanediammonium), with higher thermal stability, which also has a poor efficiency (0.027%).[260]

4.3 Other Metals

Apart from the extensive investigation of Sn and Bi, some other metal cations are also explored, mainly in IIA, IV and V groups. Krishnamoorthy *et al*. used DFT calculation to map all divalent cation AMX_3 (A: K, Rb, Cs; X: Cl, Br, I; M: 40 kinds of divalent cations) to scrutinize their bandgap and thermodynamic stability.[261] The results show that only $RbSnBr_3$, $CsSnBr_3$ and $CsGeI_3$ are suitable to apply in solar cells and $CsGeI_3$ has the most ideal bandgap of 1.6 eV. Unfortunately, the solar cells based on $CsGeI_3$ have a poor efficiency of 0.20% with low V_{oc}. Körbel *et al*. also study 32000 potential perovskites by screening the whole periodic table and a similar result, that only group IV halides are promise for photovoltaic, is obtained.[262] For organic-inorganic perovskite $AGeI_3$, its bandgap would increase as the radius of A^+ increase. Among $MAGeX_3$ (X: Cl, Br, I), $MAGeI_3$ is the most potential one for its similar property to $MAPbI_3$.[263] However, Ge^{2+} is even more sensitive to oxygen than Sn^{2+}, which is not practical for application. Similar to bismuth, antimony-based perovskite $Cs_3Sb_3I_9$ is also investigated, which, different from MBI, is a 2D layer perovskite rather than 0D perovskite (**Figure 14a-b**). [264] This material is a red powder with a bandgap of 2.05 eV. Although the DFT results imply that VBM and CBM of $Cs_3Sb_3I_9$ are similar to $MAPbI_3$, it possesses deep trap states, rendering a bad performance of its devices.

The divalent cation Sr^{2+} and Ca^{2+} in the IIA group can also form perovskite, which would be much more chemically stable than Sn^{2+} and Ge^{2+}. However, both $CH_3NH_3SrI_3$ and $CH_3NH_3CaI_3$ have a large bandgap above 3.5 eV.[265,266] The DFT calculation implies that the lack of lone pair electrons in the outer s orbital in the case of Sr^{2+} and Ca^{2+} makes their electronic structure and bandgap is dramatically different from $MAPbI_3$.[265, 266]

Another kind of lead-free perovskite reported is the Cu-based perovskite $(RNH_3)_2CuX_4$ (X: Br, Cl). According to the Goldschmidt tolerance factor, Cu-based perovskite can only form 2D perovskite owing to the smaller radius of Cu^{2+} cation. Besides, due to the redox reaction between Cu^{2+} and I^-, no cupric iodide perovskite can be formed. Cui *et al*. [267] reported two 2D perovskite, $(p\text{-}F\text{-}C_6H_5C_2H_4\text{-}NH_3)_2CuBr_4$ and $(CH_3(CH_2)_3NH_3)_2\text{-}CuBr_4$, and get efficiency of 0.51% and 0.63% for the solar cells based on them. Cortecchia *et al*. [268] fabricated a solar cell based on $MA_2CuCl_xBr_{4-x}$ with an efficiency of 0.017%. Also, they found that the octahedra CuX_6 would distort because of the Jahn-Teller effect, resulting in a worse performance (**Figure 14c**). Moreover, the reduction of Cu^{2+} may also be a problem. Although incorporating a small amount of $CuBr_2$ into $MAPbI_3$ is proved to improve the morphology and efficiency, whether Cu^{2+} actually substitute part of Pb^{2+} is unclear.[269]

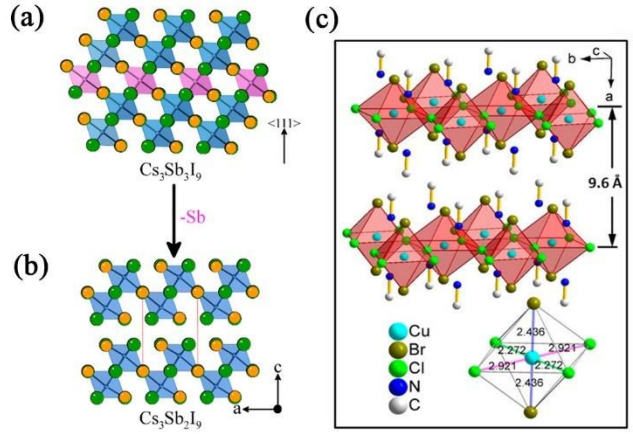

Figure 14 Removal of every third Sb layer along the ⟨111⟩ direction of (a) the perovskite structure results in (b) the 2D layered of $Cs_3Sb_2I_9$.[264] (c) Crystal structure of $MA_2CuCl_2Br_2$ and the Cu−X bond lengths.[268] Adapted with permission from ref. [264] and [268] Copyright 2016 American Chemical Society.

The recent studies of lead-free perovskite materials have implied that the performance of PVSCs is very sensitive to the presence of Pb^{2+} ion. With the simple substitution of lead to other metal cations, new perovskites generally showed the significant decline of device efficiency. Only the mixed Pb-Sn perovskites can retain a fairly high efficiency. The perovskite with mixed metal cations and halide double perovskites with 3D structure seems good in charge transport, but more research is needed. Overall, there are many identified and more on the unidentified challenges to be addressed on the development of lead-free materials with competitive performance to those of Pb-based perovskites.

5. Conclusion and Perspective

In conclusion, the rapid progresses of PVSCs have been achieved, with the improved PCEs from 3.8 % to 22.1 % in just seven years, which is never witnessed in other solar cell technologies. A great number of research efforts from community have been devoted to address a variety of issues for advancing PVSCs. Due to the limited space of this review article, we focus on mainly three aspects of recent progresses made for PVSCs, high efficiency, stability and lead-free issues. At current stage, high efficiency of PVSC has reached the level to validate its practical relevance in solar-to-electricity conversion, but it results no doubt that the device operational stability and scale-up strategies remain as challenges. On the other hand, the environmentally benign materials should be desirable that can replace lead halide perovskites with comparable performance for the long run. We suggest that more determinations on the integrative exploration of above issues are needed in order to accomplish high-performance, stable and low-cost PVSCs.

As for the PVSC efficiency, it is the outcome of the fine tuning of perovskite itself, film-formation, and interface, as well as the device architecture. Currently, although the highest certified PCE of PVSCs surpassed 22% in small areas, the continuous efforts are needed in order to fabricate large area high quality perovskite film with good reproducibility, and to clarify the design rule for efficient perovskite composition. In the meanwhile, multifunctional interfacial materials are also desired, especially for those which can interplay with perovskite crystal growth and defects passivation, as well as function as protection barriers for perovskites. Tandem devices that combine cost-effective PVSCs with low bandgap silicon or CIGS solar cells may be suitable for further improving efficiency ceilings, as well as an option for deploying PVSC into communities to be complementary with the established solar cell technologies.

The concerns on efficiency have been alleviated, but stability and the toxicity of lead remain big challenges. Chemical and structural instability of perovskite materials are the main culprit of the vulnerability for device operational stabilities. The compositional engineering of perovskites showed the encouraging progresses to address such issues. Although some materials are fairly stable within a few months, there is still a distance to make them and the related devices stable into decades under environmental stresses. Can the suitable ion substituents and/or 2D perovskites enhance the stability of materials without sacrificing efficiency? More delicate studies are needed. Device approaches such as blocking layers and encapsulation are also needed to tackle these issues. With optimism minds, the stabilities for PVSC may eventually allow reaching the prerequisites for practical application.

At current stage, studies of lead-free perovskites implied the simple substitution of lead to other metal cations in new perovskites usually led to decline device efficiency. Although Sn-Pb based perovskites promises a fairly high efficiency, Sn faces unstable issues and some reports indicate that Sn even has larger impact to human and environment than that of Pb.[224, 225] Alternatively, Bi-based halide double perovskite would be worth to pay more attention with, because it has 3D structure with good stability, as well as Bi displays a similar electronic structure to Pb. To address environmental issues of PVSCs, attentions can also be involved to develop excellent capsulation and recycling of PVSCs for avoiding the leakage of lead. To develop lead-free perovskite with high efficiency, there remain significant challenges.

Overall, it is very encouraging to reveal that the significant progresses have already achieved for PVSCs, especially in the aspects of high-efficiency device and stable material. More efforts are still needed on the integrative exploration that combines innovative materials, devices, and scale-up strategies to further advance PVSCs, in order to accomplish stable and practical solar-to-electricity conversion with perovskites.

Acknowledgements

This research was funded by National Natural Science Foundation of China (Nos. 21674093 and 51620105006), 973 program (No. 2014CB643503) and International Science and Technology Cooperation Program of China (ISTCP) (Grant No. 2016YFE0102900). C.-Z. Li thanks the support by Zhejiang Natural Science Fund for Distinguished Young Scholars

(LR17E030001), the Young 1000 Talents Global Recruitment Program of China, and 100 Talents Program of Zhejiang University.

References

1. D. Weber, *Z. Naturforsch.*, 1978, **33b**, 1443-1445.
2. A. Poglitsch and D. Weber, *Journal of Chemical Physics*, 1987, **87**, 6373-6378.
3. G. C. Papavassiliou and I. B. Koutselas, *Synthetic Metals*, 1995, **71**, 1713-1714.
4. N. Onoda-Yamamuro, T. Matsuo and H. Suga, *Journal of Physics & Chemistry of Solids*, 1992, **53**, 935-939.
5. D. B. Mitzi, S. Wang, C. A. Feild, C. A. Chess and A. M. Guloy, *Science*, 1995, **267**, 1473-1476.
6. C. D. Dimitrakopoulos, C. R. Kagan and D. B. Mitzi, *Journal*, 2002.
7. K. C. Cd, M. Db and Dimitrakopoulos, *Science*, 1999, **286**, 945-947.
8. A. Kojima, K. Teshima, Y. Shirai and T. Miyasaka, *Journal of the American Chemical Society*, 2009, **131**, 6050-6051.
9. C. W. Tang, *Applied Physics Letters*, 1986, **48**, 183-185.
10. G. Yu, J. Gao, J. C. Hummelen, F. Wudl and A. J. Heeger, *Science*, 1995, **270**, 1789-1791.
11. B. O'Regan and M. Gratzel, *Nature*, 1991, **353**, 737-740.
12. J. Xu, Y. Chen and L. Dai, *Nature Communications*, 2015, **6**, 8103.
13. http://www.nrel.gov/ncpv/images/efficiency_chart.jpg.
14. G. Xing, N. Mathews, S. Sun, S. S. Lim, Y. M. Lam, M. Grätzel, S. Mhaisalkar and T. C. Sum, *Science*, 2013, **342**, 344-347.
15. Q. Dong, Y. Fang, Y. Shao, P. Mulligan, J. Qiu, L. Cao and J. Huang, *Science*, 2015, **347**, 967-970.
16. S. D. Stranks, G. E. Eperon, G. Grancini, C. Menelaou, M. J. P. Alcocer, T. Leijtens, L. M. Herz, A. Petrozza and H. J. Snaith, *Science*, 2013, **342**, 341-344.
17. D. W. de Quilettes, S. M. Vorpahl, S. D. Stranks, H. Nagaoka, G. E. Eperon, M. E. Ziffer, H. J. Snaith and D. S. Ginger, *Science*, 2015, **348**, 683-686.
18. Q. Dong, Y. Fang, Y. Shao, P. Mulligan, J. Qiu, L. Cao and J. Huang, *Science*, 2015, **347**, 967-970.
19. C. Wehrenfennig, G. E. Eperon, M. B. Johnston, H. J. Snaith and L. M. Herz, *Advanced Materials*, 2014, **26**, 1584-1589.
20. Q. Lin, A. Armin, R. C. R. Nagiri, P. L. Burn and P. Meredith, *Nat Photon*, 2015, **9**, 106-112.
21. V. D'Innocenzo, G. Grancini, M. J. P. Alcocer, A. R. S. Kandada, S. D. Stranks, M. M. Lee, G. Lanzani, H. J. Snaith and A. Petrozza, *Nature Communications*, 2014, **5**, 3586.
22. J.-H. Im, C.-R. Lee, J.-W. Lee, S.-W. Park and N.-G. Park, *Nanoscale*, 2011, **3**, 4088-4093.
23. H.-S. Kim, C.-R. Lee, J.-H. Im, K.-B. Lee, T. Moehl, A. Marchioro, S.-J. Moon, R. Humphry-Baker, J.-H. Yum, J. E. Moser, M. Grätzel and N.-G. Park, *Scientific Reports*, 2012, **2**, 591.
24. M. M. Lee, J. Teuscher, T. Miyasaka, T. N. Murakami and H. J. Snaith, *Science*, 2012, **338**, 643-647.
25. C. Zuo, H. J. Bolink, H. Han, J. Huang, D. Cahen and L. Ding, *Adv. Sci.*, 2016, **3**, 1500324.
26. M. Saba, F. Quochi, A. Mura and G. Bongiovanni, *Accounts of Chemical Research*, 2016, **49**, 166-173.
27. L. Meng, J. You, T.-F. Guo and Y. Yang, *Accounts of Chemical Research*, 2016, **49**, 155-165. View Article Online DOI: 10.1039/C7TA00366H
28. J. S. Manser, M. I. Saidaminov, J. A. Christians, O. M. Bakr and P. V. Kamat, *Accounts of Chemical Research*, 2016, **49**, 330-338.
29. M. B. Johnston and L. M. Herz, *Accounts of Chemical Research*, 2015, **49**, 146-154.
30. S. Kazim, M. K. Nazeeruddin, M. Grätzel and S. Ahmad, *Angewandte Chemie International Edition*, 2014, **53**, 2812-2824.
31. P. Gao, M. Grätzel and M. K. Nazeeruddin, *Energy & Environmental Science*, 2014, **7**, 2448-2463.
32. T. C. Sum and N. Mathews, *Energy & Environmental Science*, 2014, **7**, 2518-2534.
33. S. D. Stranks, P. K. Nayak, W. Zhang, T. Stergiopoulos and H. J. Snaith, *Angewandte Chemie International Edition*, 2015, **54**, 3240-3248.
34. C. C. Stoumpos and M. G. Kanatzidis, *Accounts of chemical research*, 2015, **48**, 2791-2802.
35. B. V. Lotsch, *Angewandte Chemie International Edition*, 2014, **53**, 635-637.
36. Z. Wang, Z. Shi, T. Li, Y. Chen and W. Huang, *Angewandte Chemie International Edition*, 2016, DOI: 10.1002/anie.201603694.
37. F. Giustino and H. J. Snaith, *ACS Energy Letters*, 2016, **1**, 1233-1240.
38. T. A. Berhe, W.-N. Su, C.-H. Chen, C.-J. Pan, J.-H. Cheng, H.-M. Chen, M.-C. Tsai, L.-Y. Chen, A. A. Dubale and B.-J. Hwang, *Energy Environ. Sci.*, 2016, **9**, 323-356.
39. G. E. Eperon, T. Leijtens, K. A. Bush, R. Prasanna, T. Green, J. T. Wang, D. P. McMeekin, G. Volonakis, R. L. Milot, R. May, A. Palmstrom, D. J. Slotcavage, R. A. Belisle, J. B. Patel, E. S. Parrott, R. J. Sutton, W. Ma, F. Moghadam, B. Conings, A. Babayigit, H. G. Boyen, S. Bent, F. Giustino, L. M. Herz, M. B. Johnston, M. D. McGehee and H. J. Snaith, *Science*, 2016, **354**, 861-865.
40. T. Jesper Jacobsson, J.-P. Correa-Baena, M. Pazoki, M. Saliba, K. Schenk, M. Gratzel and A. Hagfeldt, *Energy & Environmental Science*, 2016, **9**, 1706-1724.
41. N. J. Jeon, J. H. Noh, W. S. Yang, Y. C. Kim, S. Ryu, J. Seo and S. I. Seok, *Nature*, 2015, **517**, 476-480.
42. H. Zhang, J. Shi, X. Xu, L. Zhu, Y. Luo, D. Li and Q. Meng, 2016, **4**, 15383-15389.
43. H. Kim, K.-G. Lim and T.-W. Lee, *Energy & Environmental Science*, 2016, **9**, 12-30.
44. C.-Z. Li, H.-L. Yip and A. K. Y. Jen, *Journal of Materials Chemistry*, 2012, **22**, 4161-4177.
45. H.-L. Yip and A. K. Y. Jen, *Energy & Environmental Science*, 2012, **5**, 5994-6011.
46. C.-C. Chueh, C.-Z. Li and A. K. Y. Jen, *Energy & Environmental Science*, 2015, **8**, 1160-1189.
47. C. D. Bailie and M. D. McGehee, *Mrs Bulletin*, 2015, **40**, 681-686.
48. T. Liu, K. Chen, Q. Hu, R. Zhu and Q. Gong, *Advanced Energy Materials*, 2016, **6**.
49. L. Meng, J. You, T.-F. Guo and Y. Yang, *Accounts of Chemical Research*, 2015, **49**, 155-165.
50. W. J. Potscavage, A. Sharma and B. Kippelen, *Accounts of Chemical Research*, 2009, **42**, 1758-1767.
51. P. W. M. Blom, V. D. Mihailetchi, L. J. A. Koster and D. E. Markov, *Advanced Materials*, 2007, **19**, 1551-1566.

52. M. Liu, M. B. Johnston and H. J. Snaith, *Nature*, 2013, **501**, 395-398.
53. J. Y. Jeng, Y. F. Chiang, M. H. Lee, S. R. Peng, T. F. Guo, P. Chen and T. C. Wen, *Advanced Materials*, 2013, **25**, 3727-3732.
54. M. Liu, M. B. Johnston and H. J. Snaith, *Nature*, 2013, **501**, 395-398.
55. C. Momblona, L. Gil-Escrig, E. Bandiello, E. M. Hutter, M. Sessolo, K. Lederer, J. Blochwitz-Nimoth and H. J. Bolink, *Energy & Environmental Science*, 2016, **9**, 3456-3463.
56. N. J. Jeon, J. H. Noh, Y. C. Kim, W. S. Yang, S. Ryu and S. I. Seok, *Nature Materials*, 2014, **13**, 897-903.
57. W. S. Yang, J. H. Noh, N. J. Jeon, Y. C. Kim, S. Ryu, J. Seo and S. I. Seok, *Science*, 2015, **348**, 1234-1237.
58. W. Li, J. Fan, J. Li, Y. Mai and L. Wang, *J Am Chem Soc*, 2015, **137**, 10399-10405.
59. W. Fu, J. Yan, Z. Zhang, T. Ye, Y. Liu, J. Wu, J. Yao, C.-Z. Li, H. Li and H. Chen, *Solar Energy Materials and Solar Cells*, 2016, **155**, 331-340.
60. F. Huang, Y. Dkhissi, W. Huang, M. Xiao, I. Benesperi, S. Rubanov, Y. Zhu, X. Lin, L. Jiang, Y. Zhou, A. Gray-Weale, J. Etheridge, C. R. McNeill, R. A. Caruso, U. Bach, L. Spiccia and Y.-B. Cheng, *Nano Energy*, 2014, **10**, 10-18.
61. J. Burschka, N. Pellet, S.-J. Moon, R. Humphry-Baker, P. Gao, M. K. Nazeeruddin and M. Grätzel, *Nature*, 2013, **499**, 316-319.
62. Z. Xiao, C. Bi, Y. Shao, Q. Dong, Q. Wang, Y. Yuan, C. Wang, Y. Gao and J. Huang, *Energy & Environmental Science*, 2014, **7**, 2619-2623.
63. Z. Xiao, Q. Dong, C. Bi, Y. Shao, Y. Yuan and J. Huang, *Advanced Materials*, 2014, **26**, 6503-6509.
64. D. Bi, C. Yi, J. Luo, J.-D. Décoppet, F. Zhang, Shaik M. Zakeeruddin, X. Li, A. Hagfeldt and M. Grätzel, *Nature Energy*, 2016, **1**, 16142.
65. Y. Liu, Q. Chen, H.-S. Duan, H. Zhou, Y. Yang, H. Chen, S. Luo, T.-B. Song, L. Dou, Z. Hong and Y. Yang, *Journal of Materials Chemistry A*, 2015, **3**, 11940-11947.
66. Y. Deng, Q. Dong, C. Bi, Y. Yuan and J. Huang, *Advanced Energy Materials*, 2016, **6**, 1600372.
67. Z. Gu, L. Zuo, T. T. Larsen-Olsen, T. Ye, G. Wu, F. C. Krebs and H. Chen, *Journal of Materials Chemistry A*, 2015, **3**, 24254-24260.
68. T. M. Schmidt, T. T. Larsen-Olsen, J. E. Carlé, D. Angmo and F. C. Krebs, *Advanced Energy Materials*, 2015, **5**, 1500569.
69. B. Conings, A. Babayigit, M. T. Klug, S. Bai, N. Gauquelin, N. Sakai, J. T.-W. Wang, J. Verbeeck, H.-G. Boyen and H. J. Snaith, *Advanced Materials*, 2016, **28**, 10701-10709.
70. F. Ye, H. Chen, F. Xie, W. Tang, M. Yin, J. He, E. Bi, Y. Wang, X. Yang and L. Han, *Energy & Environmental Science*, 2016, **9**, 2295-2301.
71. N. Ahn, D.-Y. Son, I.-H. Jang, S. M. Kang, M. Choi and N.-G. Park, *Journal of the American Chemical Society*, 2015, **137**, 8696-8699.
72. T.-B. Song, Q. Chen, H. Zhou, C. Jiang, H.-H. Wang, Y. Yang, Y. Liu, J. You and Y. Yang, *Journal of Materials Chemistry A*, 2015, **3**, 9032-9050.
73. C. Eames, J. M. Frost, P. R. F. Barnes, B. C. O'Regan, A. Walsh and M. S. Islam, *Nature Communications*, 2015, **6**, 7497.
74. H. D. Kim, H. Ohkita, H. Benten and S. Ito, *Advanced Materials*, 2015, **28**, 917-922.
75. M. Saliba, T. Matsui, K. Domanski, J.-Y. Seo, A. Ummadisingu, S. M. Zakeeruddin, J.-P. Correa-Baena, W. R. Tress, A. Abate, A. Hagfeldt and M. Grätzel, *Science*, 2016, **354**, 206-209.
76. G. E. Eperon, S. D. Stranks, C. Menelaou, M. B. Johnston, L. M. Herz and H. J. Snaith, *Energy & Environmental Science*, 2014, **7**, 982.
77. Z. Yang, A. Rajagopal, S. B. Jo, C.-C. Chueh, S. Williams, C.-C. Huang, J. K. Katahara, H. W. Hillhouse and A. K. Y. Jen, *Nano Letters*, 2016, **16**, 7739-7747.
78. J. H. Heo and S. H. Im, *Advanced Materials*, 2015, **28**, 5121-5125.
79. M. Saliba, S. Orlandi, T. Matsui, S. Aghazada, M. Cavazzini, J.-P. Correa-Baena, P. Gao, R. Scopelliti, E. Mosconi, K.-H. Dahmen, F. De Angelis, A. Abate, A. Hagfeldt, G. Pozzi, M. Graetzel and M. K. Nazeeruddin, *Nature Energy*, 2016, 15017.
80. W. Tress, N. Marinova, T. Moehl, S. M. Zakeeruddin, M. K. Nazeeruddin and M. Grätzel, 2015, **8**, 995-1004.
81. H.-S. Kim and N.-G. Park, *The Journal of Physical Chemistry Letters*, 2014, **5**, 2927-2934.
82. J. Wei, Y. Zhao, H. Li, G. Li, J. Pan, D. Xu, Q. Zhao and D. Yu, *The Journal of Physical Chemistry Letters*, 2014, **5**, 3937-3945.
83. H.-W. Chen, N. Sakai, M. Ikegami and T. Miyasaka, *The Journal of Physical Chemistry Letters*, 2015, **6**, 164-169.
84. Y. Shao, Z. Xiao, C. Bi, Y. Yuan and J. Huang, *Nature Communications*, 2014, **5**, 5784.
85. B. Chen, M. Yang, X. Zheng, C. Wu, W. Li, Y. Yan, J. Bisquert, G. Garcia-Belmonte, K. Zhu and S. Priya, *The Journal of Physical Chemistry Letters*, 2015, **6**, 4693-4700.
86. J. Zhao, X. Zheng, Y. Deng, T. Li, Y. Shao, A. Gruverman, J. Shield and J. Huang, *Energy & Environmental Science*, 2016, **9**, 3650-3656.
87. Y. Yu, C. Wang, C. R. Grice, N. Shrestha, J. Chen, D. Zhao, W. Liao, A. J. Cimaroli, P. J. Roland, R. J. Ellingson and Y. Yan, *ChemSusChem*, 2016, **9**, 3288-3297.
88. X. Li, D. Bi, C. Yi, J. D. Decoppet, J. Luo, S. M. Zakeeruddin, A. Hagfeldt and M. Gratzel, *Science*, 2016, **353**, 58-62.
89. M. Saliba, T. Matsui, J.-Y. Seo, K. Domanski, J.-P. Correa-Baena, M. K. Nazeeruddin, S. M. Zakeeruddin, W. Tress, A. Abate, A. Hagfeldt and M. Grätzel, *Energy & Environmental Science*, 2016, **9**, 1989-1997.
90. F. Ullah, H. Chen and C.-Z. Li, *Chinese Chemical Letters*, 2016, DOI: 10.1016/j.cclet.2016.11.009.
91. Z. Zhu, Y. Bai, X. Liu, C.-C. Chueh, S. Yang and A. K. Y. Jen, *Advanced Materials*, 2016, **28**, 6478-6484.
92. S. Yang, W. Liu, L. Zuo, X. Zhang, T. Ye, J. Chen, C.-Z. Li, G. Wu and H. Chen, *J. Mater. Chem. A*, 2016, **4**, 9430-9436.
93. K. Yao, X. Wang, Y.-x. Xu, F. Li and L. Zhou, *Chemistry of Materials*, 2016, **28**, 3131-3138.
94. R. Fan, Y. Huang, L. Wang, L. Li, G. Zheng and H. Zhou, *Advanced Energy Materials*, 2016, **6**, 1600460.
95. Y. Lin, L. Shen, J. Dai, Y. Deng, Y. Wu, Y. Bai, X. Zheng, J. Wang, Y. Fang, H. Wei, W. Ma, X. C. Zeng, X. Zhan and J. Huang, *Adv Mater*, 2016, DOI: 10.1002/adma.201604545.
96. Q. Dong, J. Song, Y. Fang, Y. Shao, S. Ducharme and J. Huang, *Advanced Materials*, 2016, **28**, 2816-2821.
97. C. Bi, Q. Wang, Y. Shao, Y. Yuan, Z. Xiao and J. Huang, *Nature communications*, 2015, **6**, 7747.
98. R. S. Sanchez and E. Mas-Marza, *Solar Energy Materials and Solar Cells*, 2016, **158**, 189-194.

99. Y. Yue, N. Salim, Y. Wu, X. Yang, A. Islam, W. Chen, J. Liu, E. Bi, F. Xie, M. Cai and L. Han, *Adv Mater*, 2016, **28**, 10738-10743.
100. Z. Yu and L. Sun, *Advanced Energy Materials*, 2015, **5**, 1500213.
101. Z. Li, Z. Zhu, C. C. Chueh, S. B. Jo, J. Luo, S. H. Jang and A. K. Jen, *J Am Chem Soc*, 2016, **138**, 11833-11839.
102. Z. a. Li, Z. Zhu, C.-C. Chueh, J. Luo and A. K. Y. Jen, *Advanced Energy Materials*, 2016, **6**, 1601165.
103. B. Xu, D. Bi, Y. Hua, P. Liu, M. Cheng, M. Grätzel, L. Kloo, A. Hagfeldt and L. Sun, *Energy Environ. Sci.*, 2016, **9**, 873-877.
104. T. Malinauskas, M. Saliba, T. Matsui, M. Daskeviciene, S. Urnikaite, P. Gratia, R. Send, H. Wonneberger, I. Bruder, M. Graetzel, V. Getautis and M. K. Nazeeruddin, *Energy Environ. Sci.*, 2016, **9**, 1681-1686.
105. M. Saliba, S. Orlandi, T. Matsui, S. Aghazada, M. Cavazzini, J.-P. Correa-Baena, P. Gao, R. Scopelliti, E. Mosconi, K.-H. Dahmen, F. De Angelis, A. Abate, A. Hagfeldt, G. Pozzi, M. Graetzel and M. K. Nazeeruddin, *Nature Energy*, 2016, **1**, 15017.
106. H. Nishimura, N. Ishida, A. Shimazaki, A. Wakamiya, A. Saeki, L. T. Scott and Y. Murata, *J Am Chem Soc*, 2015, **137**, 15656-15659.
107. Q. Xue, G. Chen, M. Liu, J. Xiao, Z. Chen, Z. Hu, X.-F. Jiang, B. Zhang, F. Huang, W. Yang, H.-L. Yip and Y. Cao, *Advanced Energy Materials*, 2016, **6**, 1502021.
108. K.-T. Lee, L. J. Guo and H. J. Park, *Molecules*, 2016, **21**, 475.
109. D. Zhao, M. Sexton, H.-Y. Park, G. Baure, J. C. Nino and F. So, *Advanced Energy Materials*, 2015, **5**, 1401855.
110. S. Ryu, J. H. Noh, N. J. Jeon, Y. Chan Kim, W. S. Yang, J. Seo and S. I. Seok, *Energy & Environmental Science*, 2014, **7**, 2614-2618.
111. C. Huang, W. Fu, C. Z. Li, Z. Zhang, W. Qiu, M. Shi, P. Heremans, A. K. Jen and H. Chen, *J Am Chem Soc*, 2016, **138**, 2528-2531.
112. K. C. Wang, J. Y. Jeng, P. S. Shen, Y. C. Chang, E. W. Diau, C. H. Tsai, T. Y. Chao, H. C. Hsu, P. Y. Lin, P. Chen, T. F. Guo and T. C. Wen, *Scientific reports*, 2014, **4**, 4756.
113. Z. Zhu, Y. Bai, T. Zhang, Z. Liu, X. Long, Z. Wei, Z. Wang, L. Zhang, J. Wang, F. Yan and S. Yang, *Angewandte Chemie*, 2014, **53**, 12571-12575.
114. J. You, L. Meng, T. B. Song, T. F. Guo, Y. M. Yang, W. H. Chang, Z. Hong, H. Chen, H. Zhou, Q. Chen, Y. Liu, N. De Marco and Y. Yang, *Nature nanotechnology*, 2016, **11**, 75-81.
115. J. W. Jung, C. C. Chueh and A. K. Jen, *Adv Mater*, 2015, **27**, 7874-7880.
116. H. Zhang, H. Wang, W. Chen and A. K. Jen, *Adv Mater*, 2016, DOI: 10.1002/adma.201604984.
117. Z.-K. Yu, W.-F. Fu, W.-Q. Liu, Z.-Q. Zhang, Y.-J. Liu, J.-L. Yan, T. Ye, W.-T. Yang, H.-Y. Li and H.-Z. Chen, *Chinese Chemical Letters*, 2016.
118. Y. Zhao and K. Zhu, *Chemical Society reviews*, 2016, **45**, 655-689.
119. K. Wojciechowski, S. D. Stranks, A. Abate, G. Sadoughi, A. Sadhanala, N. Kopidakis, G. Rumbles, C.-Z. Li, R. H. Friend, A. K. Y. Jen and H. J. Snaith, *ACS Nano*, 2014, **8**, 12701-12709.
120. K. Wojciechowski, T. Leijtens, S. Siprova, C. Schlueter, M. T. Horantner, J. T. Wang, C. Z. Li, A. K. Jen, T. L. Lee and H. J. Snaith, *J Phys Chem Lett*, 2015, **6**, 2399-2405.
121. T. Salim, S. Sun, Y. Abe, A. Krishna, A. C. Grimsdale and Y. M. Lam, *J. Mater. Chem. A*, 2015, **3**, 8943-8969.
122. P. W. Liang, C. Y. Liao, C. C. Chueh, F. Zuo, S. T. Williams, X. K. Xin, J. Lin and A. K. Jen, *Adv Mater*, 2014, **26**, 3748-3754.
123. O. Malinkiewicz, A. Yella, Y. H. Lee, G. M. Espallargas, M. Graetzel, M. K. Nazeeruddin and H. J. Bolink, *Nature Photonics*, 2013, **8**, 128-132.
124. Z. Zhu, C. C. Chueh, F. Lin and A. K. Jen, *Adv Sci (Weinh)*, 2016, **3**, 1600027.
125. P.-W. Liang, C.-C. Chueh, S. T. Williams and A. K. Y. Jen, *Advanced Energy Materials*, 2015, **5**, 1402321.
126. H. Zhou, Q. Chen, G. Li, S. Luo, T.-b. Song, H.-S. Duan, Z. Hong, J. You, Y. Liu and Y. Yang, *Science*, 2014, **345**, 542-546.
127. X. Liu, K.-W. Tsai, Z. Zhu, Y. Sun, C.-C. Chueh and A. K. Y. Jen, *Advanced Materials Interfaces*, 2016, **3**, 1600122.
128. J. P. Correa Baena, L. Steier, W. Tress, M. Saliba, S. Neutzner, T. Matsui, F. Giordano, T. J. Jacobsson, A. R. Srimath Kandada, S. M. Zakeeruddin, A. Petrozza, A. Abate, M. K. Nazeeruddin, M. Grätzel and A. Hagfeldt, *Energy Environ. Sci.*, 2015, **8**, 2928-2934.
129. L. Zuo, Z. Gu, T. Ye, W. Fu, G. Wu, H. Li and H. Chen, *J Am Chem Soc*, 2015, **137**, 2674-2679.
130. G. Grancini, R. S. Santosh Kumar, A. Abrusci, H.-L. Yip, C.-Z. Li, A.-K. Y. Jen, G. Lanzani and H. J. Snaith, *Advanced Functional Materials*, 2012, **22**, 2160-2166.
131. J. Cui, P. Li, Z. Chen, K. Cao, D. Li, J. Han, Y. Shen, M. Peng, Y. Q. Fu and M. Wang, *Applied Physics Letters*, 2016, **109**, 171103.
132. J. Huang, X. Zhang, D. Zheng, K. Yan, C.-Z. Li and J. Yu, *Solar RRL*, 2017, DOI: 10.1002/solr.201600008, 1600008.
133. M. Valles-Pelarda, B. C. Hames, I. García-Benito, O. Almora, A. Molina-Ontoria, R. S. Sánchez, G. Garcia-Belmonte, N. Martín and I. Mora-Sero, *The Journal of Physical Chemistry Letters*, 2016, **7**, 4622-4628.
134. A. Abrusci, S. D. Stranks, P. Docampo, H.-L. Yip, A. K. Y. Jen and H. J. Snaith, *Nano Letters*, 2013, **13**, 3124-3128.
135. J. Huang, X. Yu, J. Xie, C.-Z. Li, Y. Zhang, D. Xu, Z. Tang, C. Cui and D. Yang, *ACS Applied Materials & Interfaces*, 2016, **8**, 34612-34619.
136. C.-Y. Chang, W.-K. Huang, Y.-C. Chang, K.-T. Lee and H.-Y. Siao, *Chem. Mat.*, 2015, **27**, 1869-1875.
137. J. Xie, X. Yu, X. Sun, J. Huang, Y. Zhang, M. Lei, K. Huang, D. Xu, Z. Tang, C. Cui and D. Yang, *Nano Energy*, 2016, **28**, 330-337.
138. C.-Y. Chang, W.-K. Huang, Y.-C. Chang, K.-T. Lee and C.-T. Chen, *J. Mater. Chem. A*, 2016, **4**, 640-648.
139. C.-Y. Chang, W.-K. Huang and Y.-C. Chang, *Chem. Mat.*, 2016, **28**, 6305-6312.
140. Y. Xing, C. Sun, H. L. Yip, G. C. Bazan, F. Huang and Y. Cao, *Nano Energy*, 2016, **26**, 7-15.
141. S. Shao, M. Abdu-Aguye, L. Qiu, L.-H. Lai, J. Liu, S. Adjokatse, F. Jahani, M. E. Kamminga, G. H. ten Brink, T. T. M. Palstra, B. J. Kooi, J. C. Hummelen and M. Antonietta Loi, *Energy Environ. Sci.*, 2016, **9**, 2444-2452.
142. X. Liu, M. Lei, Y. Zhou, B. Song and Y. Li, *Applied Physics Letters*, 2015, **107**, 063901.

143. C. Z. Li, C. C. Chueh, H. L. Yip, F. Ding, X. Li and A. K. Jen, *Adv Mater*, 2013, **25**, 2457-2461.
144. C. Z. Li, C. C. Chueh, F. Ding, H. L. Yip, P. W. Liang, X. Li and A. K. Jen, *Adv Mater*, 2013, **25**, 4425-4430.
145. B. Zhao, C.-Z. Li, S.-Q. Liu, J. J. Richards, C.-C. Chueh, F. Ding, L. D. Pozzo, X. Li and A. K. Y. Jen, *J. Mater. Chem. A*, 2015, **3**, 6929-6934.
146. C.-Z. Li, C.-C. Chueh, H.-L. Yip, K. M. O'Malley, W.-C. Chen and A. K. Y. Jen, *Journal of Materials Chemistry*, 2012, **22**, 8574.
147. C.-Z. Li, P.-W. Liang, D. B. Sulas, P. D. Nguyen, X. Li, D. S. Ginger, C. W. Schlenker and A. K. Y. Jen, *Mater. Horiz.*, 2015, **2**, 414-419.
148. Z. Zhu, C.-C. Chueh, G. Zhang, F. Huang, H. Yan and A. K. Y. Jen, *ChemSusChem*, 2016, **9**, 2586-2591.
149. C. Sun, Z. Wu, H.-L. Yip, H. Zhang, X.-F. Jiang, Q. Xue, Z. Hu, Z. Hu, Y. Shen, M. Wang, F. Huang and Y. Cao, *Advanced Energy Materials*, 2016, **6**, 1501534.
150. S. Zhang, Z. Yu, P. Li, B. Li, F. H. Isikgor, D. Du, K. Sun, Y. Xia and J. Ouyang, *Organic Electronics*, 2016, **32**, 149-156.
151. W. Zhu, C. Bao, F. Li, T. Yu, H. Gao, Y. Yi, J. Yang, G. Fu, X. Zhou and Z. Zou, *Nano Energy*, 2016, **19**, 17-26.
152. W. Liu, S. Li, J. Huang, S. Yang, J. Chen, L. Zuo, M. Shi, X. Zhan, C. Z. Li and H. Chen, *Adv. Mater.*, 2016, **28**, 9729–9734.
153. A. R. b. M. Yusoff, D. Kim, H. P. Kim, F. K. Shneider, W. J. da Silva and J. Jang, *Energy Environ. Sci.*, 2015, **8**, 303-316.
154. J. You, L. Dou, K. Yoshimura, T. Kato, K. Ohya, T. Moriarty, K. Emery, C.-C. Chen, J. Gao, G. Li and Y. Yang, *Nat Commun*, 2013, **4**, 1446.
155. L. Zuo, C.-C. Chueh, Y.-X. Xu, K.-S. Chen, Y. Zang, C.-Z. Li, H. Chen and A. K. Y. Jen, *Adv. Mater.*, 2014, **26**, 6778-6784.
156. F. Hao, C. C. Stoumpos, R. P. H. Chang and M. G. Kanatzidis, *Journal of the American Chemical Society*, 2014, **136**, 8094-8099.
157. J. H. Heo and S. H. Im, *Advanced Materials*, 2016, **28**, 5121-5125.
158. C. D. Bailie and M. D. McGehee, *Mrs Bull*, 2015, **40**, 681-686.
159. P. Löper, B. Niesen, S. J. Moon, S. M. d. Nicolas, J. Holovsky, Z. Remes, M. Ledinsky, F. J. Haug, J. H. Yum, S. D. Wolf and C. Ballif, *IEEE Journal of Photovoltaics*, 2014, **4**, 1545-1551.
160. D. P. McMeekin, G. Sadoughi, W. Rehman, G. E. Eperon, M. Saliba, M. T. Hörantner, A. Haghighirad, N. Sakai, L. Korte, B. Rech, M. B. Johnston, L. M. Herz and H. J. Snaith, *Science*, 2016, **351**, 151-155.
161. Z. Yang, A. Rajagopal, C.-C. Chueh, S. B. Jo, B. Liu, T. Zhao and A. K. Y. Jen, *Advanced Materials*, 2016, **28**, 8990-8997.
162. C. D. Bailie, M. G. Christoforo, J. P. Mailoa, A. R. Bowring, E. L. Unger, W. H. Nguyen, J. Burschka, N. Pellet, J. Z. Lee, M. Gratzel, R. Noufi, T. Buonassisi, A. Salleo and M. D. McGehee, *Energy & Environmental Science*, 2015, **8**, 956-963.
163. P. Loper, S. J. Moon, S. M. de Nicolas, B. Niesen, M. Ledinsky, S. Nicolay, J. Bailat, J. H. Yum, S. De Wolf and C. Ballif, *Physical Chemistry Chemical Physics*, 2015, **17**, 1619-1629.
164. K. A. Bush, C. D. Bailie, Y. Chen, A. R. Bowring, W. Wang, W. Ma, T. Leijtens, F. Moghadam and M. D. McGehee, *Advanced Materials*, 2016, **28**, 3937-3943.
165. S. Albrecht, M. Saliba, J. P. Correa Baena, F. Lang, L. Kegelmann, M. Mews, L. Steier, A. Abate, J. Rappich, L. Korte, R. Schlatmann, M. K. Nazeeruddin, A. Hagfeldt, M. Gratzel and B. Rech, *Energy & Environmental Science*, 2016, **9**, 81-88.
166. J. Werner, C.-H. Weng, A. Walter, L. Fesquet, J. P. Seif, S. De Wolf, B. Niesen and C. Ballif, *The Journal of Physical Chemistry Letters*, 2016, **7**, 161-166.
167. X. Yin, P. Chen, M. Que, Y. Xing, W. Que, C. Niu and J. Shao, *ACS Nano*, 2016, **10**, 3630-3636.
168. J. Werner, L. Barraud, A. Walter, M. Bräuninger, F. Sahli, D. Sacchetto, N. Tétreault, B. Paviet-Salomon, S.-J. Moon, C. Allebé, M. Despeisse, S. Nicolay, S. De Wolf, B. Niesen and C. Ballif, *ACS Energy Letters*, 2016, **1**, 474-480.
169. T. Todorov, T. Gershon, O. Gunawan, C. Sturdevant and S. Guha, *Applied Physics Letters*, 2014, **105**, 173902.
170. T. Todorov, T. Gershon, O. Gunawan, Y. S. Lee, C. Sturdevant, L.-Y. Chang and S. Guha, *Advanced Energy Materials*, 2015, **5**.
171. F. Fu, T. Feurer, T. Jäger, E. Avancini, B. Bissig, S. Yoon, S. Buecheler and A. N. Tiwari, *Nature Communications*, 2015, **6**, 8932.
172. C.-C. Chen, S.-H. Bae, W.-H. Chang, Z. Hong, G. Li, Q. Chen, H. Zhou and Y. Yang, *Materials Horizons*, 2015, **2**, 203-211.
173. D. Forgács, L. Gil-Escrig, D. Pérez-Del-Rey, C. Momblona, J. Werner, B. Niesen, C. Ballif, M. Sessolo and H. J. Bolink, *Advanced Energy Materials*, 2016, DOI: 10.1002/aenm.201602121, 1602121.
174. G. E. Eperon, T. Leijtens, K. A. Bush, R. Prasanna, T. Green, J. T.-W. Wang, D. P. McMeekin, G. Volonakis, R. L. Milot, R. May, A. Palmstrom, D. J. Slotcavage, R. A. Belisle, J. B. Patel, E. S. Parrott, R. J. Sutton, W. Ma, F. Moghadam, B. Conings, A. Babayigit, H.-G. Boyen, S. Bent, F. Giustino, L. M. Herz, M. B. Johnston, M. D. McGehee and H. J. Snaith, *Science*, 2016, **354**, 861-865.
175. A. Poglitsch and D. Weber, *The Journal of Chemical Physics*, 1987, **87**, 6373.
176. H. Zhou, Y. Shi, Q. Dong, H. Zhang, Y. Xing, K. Wang, Y. Du and T. Ma, *The Journal of Physical Chemistry Letters*, 2014, **5**, 3241-3246.
177. Y. Guo, K. Shoyama, W. Sato and E. Nakamura, *Advanced Energy Materials*, 2016, **6**, 1502317.
178. R. Cao, F. Xu, J. Zhu, S. Ge, W. Wang, H. Xu, R. Xu, Y. Wu, Z. Ma, F. Hong and Z. Jiang, *Advanced Energy Materials*, 2016, **6**, 1600814.
179. R. K. Misra, S. Aharon, B. Li, D. Mogilyansky, I. Visoly-Fisher, L. Etgar and E. A. Katz, *The Journal of Physical Chemistry Letters*, 2015, **6**, 326-330.
180. B. Conings, J. Drijkoningen, N. Gauquelin, A. Babayigit, J. D'Haen, L. D'Olieslaeger, A. Ethirajan, J. Verbeeck, J. Manca, E. Mosconi, F. D. Angelis and H.-G. Boyen, *Advanced Energy Materials*, 2015, **5**, 1500477.
181. D. Bryant, N. Aristidou, S. Pont, I. Sanchez-Molina, T. Chotchunangatchaval, S. Wheeler, J. R. Durrant and S. A. Haque, *Energy & Environmental Science*, 2016, **9**, 1655-1660.
182. W. Kong, A. Rahimi-Iman, G. Bi, X. Dai and H. Wu, *The Journal of Physical Chemistry C*, 2016, **120**, 7606-7611.
183. Z. Song, A. Abate, S. C. Watthage, G. K. Liyanage, A. B. Phillips, U. Steiner, M. Graetzel and M. J. Heben, *Advanced Energy Materials*, 2016, **6**, 1600846.

184. Y. Han, S. Meyer, Y. Dkhissi, K. Weber, J. M. Pringle, U. Bach, L. Spiccia and Y.-B. Cheng, *Journal of Materials Chemistry A*, 2015, **3**, 8139-8147.
185. F. Huang, L. Jiang, A. R. Pascoe, Y. Yan, U. Bach, L. Spiccia and Y.-B. Cheng, *Nano Energy*, 2016, **27**, 509-514.
186. D. Wei, T. Wang, J. Ji, M. Li, P. Cui, Y. Li, G. Li, J. M. Mbengue and D. Song, *Journal of Materials Chemistry A*, 2016, **4**, 1991-1998.
187. N. Z. Koocher, D. Saldana-Greco, F. Wang, S. Liu and A. M. Rappe, *The Journal of Physical Chemistry Letters*, 2015, **6**, 4371-4378.
188. C. Ran, Y. Chen, W. Gao, M. Wang and L. Dai, *Journal of Materials Chemistry A*, 2016, **4**, 8566-8572.
189. Y. Chen, T. Chen and L. Dai, *Advanced Materials*, 2015, **27**, 1053-1059.
190. S. Aharon, A. Dymshits, A. Rotem and L. Etgar, *J. Mater. Chem. A*, 2015, **3**, 9171-9178.
191. J.-W. Lee, D.-H. Kim, H.-S. Kim, S.-W. Seo, S. M. Cho and N.-G. Park, *Advanced Energy Materials*, 2015, **5**, 1501310.
192. C. Yi, J. Luo, S. Meloni, A. Boziki, N. Ashari-Astani, C. Grätzel, S. M. Zakeeruddin, U. Rothlisberger and M. Grätzel, *Energy & Environmental Science*, 2015, **9**, 656-662.
193. T. M. Koh, K. Fu, Y. Fang, S. Chen, T. C. Sum, N. Mathews, S. G. Mhaisalkar, P. P. Boix and T. Baikie, *The Journal of Physical Chemistry C*, 2014, **118**, 16458-16462.
194. N. Pellet, P. Gao, G. Gregori, T.-Y. Yang, M. K. Nazeeruddin, J. Maier and M. Grätzel, *Angewandte Chemie International Edition*, 2014, **53**, 3151-3157.
195. A. Binek, F. C. Hanusch, P. Docampo and T. Bein, *The Journal of Physical Chemistry Letters*, 2015, **6**, 1249-1253.
196. R. J. Sutton, G. E. Eperon, L. Miranda, E. S. Parrott, B. A. Kamino, J. B. Patel, M. T. Hörantner, M. B. Johnston, A. A. Haghighirad, D. T. Moore and H. J. Snaith, *Advanced Energy Materials*, 2016, **6**, 1502458.
197. Q. Ma, S. Huang, X. Wen, M. A. Green and A. W. Y. Ho-Baillie, *Advanced Energy Materials*, 2016, **6**, 1502202.
198. J. Liang, C. Wang, Y. Wang, Z. Xu, Z. Lu, Y. Ma, H. Zhu, Y. Hu, C. Xiao, X. Yi, G. Zhu, H. Lv, L. Ma, T. Chen, Z. Tie, Z. Jin and J. Liu, *Journal of the American Chemical Society*, 2016, **138**, 15829-15832.
199. M. Kulbak, S. Gupta, N. Kedem, I. Levine, T. Bendikov, G. Hodes and D. Cahen, *J Phys Chem Lett*, 2016, **7**, 167-172.
200. A. Swarnkar, A. R. Marshall, E. M. Sanehira, B. D. Chernomordik, D. T. Moore, J. A. Christians, T. Chakrabarti and J. M. Luther, *Science*, 2016, **354**, 92-95.
201. J. H. Noh, S. H. Im, J. H. Heo, T. N. Mandal and S. I. Seok, *Nano Letters*, 2013, **13**, 1764-1769.
202. N. Arora, M. I. Dar, M. Abdi-Jalebi, F. Giordano, N. Pellet, G. Jacopin, R. H. Friend, S. M. Zakeeruddin and M. Grätzel, *Nano Letters*, 2016, **16**, 7155-7162.
203. Y. C. Kim, N. J. Jeon, J. H. Noh, W. S. Yang, J. Seo, J. S. Yun, A. Ho-Baillie, S. Huang, M. A. Green, J. Seidel, T. K. Ahn and S. I. Seok, *Advanced Energy Materials*, 2015, **6**, 1502104.
204. Q. Jiang, D. Rebollar, J. Gong, E. L. Piacentino, C. Zheng and T. Xu, *Angewandte Chemie International Edition*, 2015, **54**, 7617-7620.
205. M. Daub and H. Hillebrecht, *Angewandte Chemie International Edition*, 2015, **54**, 11016-11017.
206. A. M. Ganose, C. N. Savory and D. O. Scanlon, *The Journal of Physical Chemistry Letters*, 2015, **6**, 4594-4598.
207. Z. Xiao, W. Meng, B. Saparov, H.-S. Duan, C. Wang, C. Feng, W. Liao, W. Ke, D. Zhao, J. Wang, D. B. Mitzi and Y. Yan, *The Journal of Physical Chemistry Letters*, 2016, **7**, 1213-1218.
208. D. Umeyama, Y. Lin and H. I. Karunadasa, *Chemistry of Materials*, 2016, **28**, 3241-3244.
209. I. C. Smith, E. T. Hoke, D. Solis-Ibarra, M. D. McGehee and H. I. Karunadasa, *Angewandte Chemie*, 2014, **53**, 11232-11235.
210. L. N. Quan, M. Yuan, R. Comin, O. Voznyy, E. M. Beauregard, S. Hoogland, A. Buin, A. R. Kirmani, K. Zhao, A. Amassian, D. H. Kim and E. H. Sargent, *Journal of the American Chemical Society*, 2016, **138**, 2649-2655.
211. H. Tsai, W. Nie, J.-C. Blancon, C. C. Stoumpos, R. Asadpour, B. Harutyunyan, A. J. Neukirch, R. Verduzco, J. J. Crochet, S. Tretiak, L. Pedesseau, J. Even, M. A. Alam, G. Gupta, J. Lou, P. M. Ajayan, M. J. Bedzyk, M. G. Kanatzidis and A. D. Mohite, *Nature*, 2016, **536**, 312-316.
212. D. Bi, P. Gao, R. Scopelliti, E. Oveisi, J. Luo, M. Grätzel, A. Hagfeldt and M. K. Nazeeruddin, *Advanced Materials*, 2016, **28**, 2910-2915.
213. Q. Wang, Q. Dong, T. Li, A. Gruverman and J. Huang, *Advanced Materials*, 2016, **28**, 6734-6739.
214. Y. Zhao, J. Wei, H. Li, Y. Yan, W. Zhou, D. Yu and Q. Zhao, *Nature Communications*, 2016, **7**, 10228.
215. D. H. Cao, C. C. Stoumpos, O. K. Farha, J. T. Hupp and M. G. Kanatzidis, *Journal of the American Chemical Society*, 2015, **137**, 7843-7850.
216. T. M. Koh, V. Shanmugam, J. Schlipf, L. Oesinghaus, P. Müller-Buschbaum, N. Ramakrishnan, V. Swamy, N. Mathews, P. P. Boix and S. G. Mhaisalkar, *Advanced Materials*, 2016, **28**, 3653-3661.
217. S. Yang, Y. Wang, P. Liu, Y.-B. Cheng, H. J. Zhao and H. G. Yang, *Nature Energy*, 2016, **1**, 15016.
218. F. Bella, G. Griffini, J. P. Correa-Baena, G. Saracco, M. Gratzel, A. Hagfeldt, S. Turri and C. Gerbaldi, *Science*, 2016, **354**, 203-206.
219. K. Domanski, J.-P. Correa-Baena, N. Mine, M. K. Nazeeruddin, A. Abate, M. Saliba, W. Tress, A. Hagfeldt and M. Grätzel, *ACS Nano*, 2016, **10**, 6306-6314.
220. H. Back, G. Kim, J. Kim, J. Kong, T. K. Kim, H. Kang, H. Kim, J. Lee, S. Lee and K. Lee, *Energy & Environmental Science*, 2016, **9**, 1258-1263.
221. A. Mei, X. Li, L. Liu, Z. Ku, T. Liu, Y. Rong, M. Xu, M. Hu, J. Chen, Y. Yang, M. Grätzel and H. Han, *Science*, 2014, **345**, 295-298.
222. Y. Rong, L. Liu, A. Mei, X. Li and H. Han, *Advanced Energy Materials*, 2015, **5**, 1501066.
223. X. Li, M. Tschumi, H. Han, S. S. Babkair, R. A. Alzubaydi, A. A. Ansari, S. S. Habib, M. K. Nazeeruddin, S. M. Zakeeruddin and M. Grätzel, *Energy Technology*, 2015, **3**, 551-555.
224. L. Serrano-Lujan, N. Espinosa, T. T. Larsen-Olsen, J. Abad, A. Urbina and F. C. Krebs, *Advanced Energy Materials*, 2015, **5**, 1501119.
225. A. Babayigit, D. Duy Thanh, A. Ethirajan, J. Manca, M. Muller, H.-G. Boyen and B. Conings, *Scientific Reports*, 2016, **6**, 18721.
226. A. Babayigit, A. Ethirajan, M. Muller and B. Conings, *Nature Materials*, 2016, **15**, 247-251.
227. A. R. b. M. Yusoff and M. K. Nazeeruddin, *The Journal of Physical Chemistry Letters*, 2016, **7**, 851-866.

228. I. Borriello, G. Cantele and D. Ninno, *Phys. Rev. B*, 2008, **77**, 235214.
229. F. Brivio, A. B. Walker and A. Walsh, *APL Materials*, 2013, **1**, 042111.
230. W.-J. Yin, J.-H. Yang, J. Kang, Y. Yan and S.-H. Wei, *Journal of Materials Chemistry A*, 2015, **3**, 8926-8942.
231. Y.-Y. Pan, Y.-H. Su, C.-H. Hsu, L.-W. Huang and C.-C. Kaun, *Computational Materials Science*, 2016, **117**, 573-578.
232. F. Hao, C. C. Stoumpos, D. H. Cao, R. P. H. Chang and M. G. Kanatzidis, *Nature Photonics*, 2014, **8**, 489-494.
233. N. K. Noel, S. D. Stranks, A. Abate, C. Wehrenfennig, S. Guarnera, A.-A. Haghighirad, A. Sadhanala, G. E. Eperon, S. K. Pathak, M. B. Johnston, A. Petrozza, L. M. Herz and H. J. Snaith, *Energy & Environmental Science*, 2014, **7**, 3061-3068.
234. F. Hao, C. C. Stoumpos, P. Guo, N. Zhou, T. J. Marks, R. P. H. Chang and M. G. Kanatzidis, *Journal of the American Chemical Society*, 2015, **137**, 11445-11452.
235. T. Yokoyama, D. H. Cao, C. C. Stoumpos, T.-B. Song, Y. Sato, S. Aramaki and M. G. Kanatzidis, *The Journal of Physical Chemistry Letters*, 2016, **7**, 776-782.
236. H. Hoshi, N. Shigeeda and T. Dai, *Materials Letters*, 2016, **183**, 391-393.
237. T. M. Koh, T. Krishnamoorthy, N. Yantara, C. Shi, W. L. Leong, P. P. Boix, A. C. Grimsdale, S. G. Mhaisalkar and N. Mathews, *Journal of Materials Chemistry A*, 2015, **3**, 14996-15000.
238. M. H. Kumar, S. Dharani, W. L. Leong, P. P. Boix, R. R. Prabhakar, T. Baikie, C. Shi, H. Ding, R. Ramesh, M. Asta, M. Graetzel, S. G. Mhaisalkar and N. Mathews, *Advanced Materials*, 2014, **26**, 7122-7127.
239. S. J. Lee, S. S. Shin, Y. C. Kim, D. Kim, T. K. Ahn, J. H. Noh, J. Seo and S. I. Seok, *Journal of the American Chemical Society*, 2016, **138**, 3974-3977.
240. C. C. Stoumpos, C. D. Malliakas and M. G. Kanatzidis, *Inorg. Chem.*, 2013, **52**, 9019-9038.
241. C. Bernal and K. Yang, *The Journal of Physical Chemistry C*, 2014, **118**, 24383-24388.
242. N. Wang, Y. Zhou, M.-G. Ju, H. F. Garces, T. Ding, S. Pang, X. C. Zeng, N. P. Padture and X. W. Sun, *Advanced Energy Materials*, 2016, **6**, n/a-n/a.
243. B. Lee, C. C. Stoumpos, N. Zhou, F. Hao, C. Malliakas, C.-Y. Yeh, T. J. Marks, M. G. Kanatzidis and R. P. H. Chang, *Journal of the American Chemical Society*, 2014, **136**, 15379-15385.
244. F. Zuo, S. T. Williams, P.-W. Liang, C.-C. Chueh, C.-Y. Liao and A. K. Y. Jen, *Advanced Materials*, 2014, **26**, 6454-6460.
245. J. Im, C. C. Stoumpos, H. Jin, A. J. Freeman and M. G. Kanatzidis, *The Journal of Physical Chemistry Letters*, 2015, **6**, 3503-3509.
246. Z. Wang, Q. Dong, Y. Xia, H. Yu, K. Zhang, X. Liu, X. Guo, Y. Zhou, M. Zhang and B. Song, *Organic Electronics*, 2016, **33**, 142-149.
247. K. Eckhardt, V. Bon, J. Getzschmann, J. Grothe, F. M. Wisser and S. Kaskel, *Chemical Communications*, 2016, **52**, 3058-3060.
248. A. J. Lehner, D. H. Fabini, H. A. Evans, C.-A. Hébert, S. R. Smock, J. Hu, H. Wang, J. W. Zwanziger, M. L. Chabinyc and R. Seshadri, *Chemistry of Materials*, 2015, **27**, 7137-7148.
249. S. Sun, S. Tominaka, J.-H. Lee, F. Xie, P. D. Bristowe and A. K. Cheetham, *APL Materials*, 2016, **4**, 031101.
250. B.-W. Park, B. Philippe, X. Zhang, H. Rensmo, G. Boschloo and E. M. J. Johansson, *Advanced Materials*, 2015, **27**.
251. R. L. Z. Hoye, R. E. Brandt, A. Osherov, V. Stevanović, S. D. Stranks, M. W. B. Wilson, H. Kim, A. J. Akey, J. D. Perkins, R. C. Kurchin, J. R. Poindexter, E. N. Wang, M. G. Bawendi, V. Bulović and T. Buonassisi, *Chemistry - A European Journal*, 2016, **22**, 2605-2610.
252. B.-W. Park, B. Philippe, X. Zhang, H. Rensmo, G. Boschloo and E. M. J. Johansson, *Advanced Materials*, 2015, **27**, 6806-6813.
253. X. Zhang, G. Wu, Z. Gu, B. Guo, W. Liu, S. Yang, T. Ye, C. Chen, W. Tu and H. Chen, *Nano Res.*, 2016, **9**, 2921-2930.
254. M. R. Filip, S. Hillman, A. A. Haghighirad, H. J. Snaith and F. Giustino, *The Journal of Physical Chemistry Letters*, 2016, **7**, 2579-2585.
255. Y. Kim, Z. Yang, A. Jain, O. Voznyy, G.-H. Kim, M. Liu, L. N. Quan, F. P. García de Arquer, R. Comin, J. Z. Fan and E. H. Sargent, *Angewandte Chemie International Edition*, 2016, **55**, 9586-9590.
256. E. T. McClure, M. R. Ball, W. Windl and P. M. Woodward, *Chemistry of Materials*, 2016, **28**, 1348-1354.
257. A. H. Slavney, T. Hu, A. M. Lindenberg and H. I. Karunadasa, *Journal of the American Chemical Society*, 2016, **138**, 2138-2141.
258. F. Wei, Z. Deng, S. Sun, F. Xie, G. Kieslich, D. M. Evans, M. A. Carpenter, P. D. Bristowe and A. K. Cheetham, *Materials Horizons*, 2016, **3**, 328-332.
259. G. Giorgi and K. Yamashita, *Chem Lett*, 2015, **44**, 826-828.
260. D. M. Fabian and S. Ardo, 2016, **4**, 6837-6841.
261. T. Krishnamoorthy, H. Ding, C. Yan, W. L. Leong, T. Baikie, Z. Zhang, M. Sherburne, S. Li, M. Asta, N. Mathews and S. G. Mhaisalkar, *Journal of Materials Chemistry A*, 2015, **3**, 23829-23832.
262. S. Körbel, M. A. L. Marques and S. Botti, 2016, **4**, 3157-3167.
263. P.-P. Sun, Q.-S. Li, L.-N. Yang and Z.-S. Li, *Nanoscale*, 2016, **8**, 1503-1512.
264. B. Saparov, F. Hong, J.-P. Sun, H.-S. Duan, W. Meng, S. Cameron, I. G. Hill, Y. Yan and D. B. Mitzi, *Chemistry of Materials*, 2015, **27**, 5622-5632.
265. T. J. Jacobsson, M. Pazoki, A. Hagfeldt and T. Edvinsson, *The Journal of Physical Chemistry C*, 2015, **119**, 25673-25683.
266. J. I. Uribe, D. Ramirez, J. M. Osorio-Guillén, J. Osorio and F. Jaramillo, *The Journal of Physical Chemistry C*, 2016, **120**, 16393-16398.
267. X.-P. Cui, K.-J. Jiang, J.-H. Huang, Q.-Q. Zhang, M.-J. Su, L.-M. Yang, Y.-L. Song and X.-Q. Zhou, *Synthetic Metals*, 2015, **209**, 247-250.
268. D. Cortecchia, H. A. Dewi, J. Yin, A. Bruno, S. Chen, T. Baikie, P. P. Boix, M. Grätzel, S. Mhaisalkar, C. Soci and N. Mathews, *Inorg. Chem.*, 2016, **55**, 1044-1052.
269. M. Jahandar, J. H. Heo, C. E. Song, K.-J. Kong, W. S. Shin, J.-C. Lee, S. H. Im and S.-J. Moon, *Nano Energy*, 2016, **27**, 330-339.

View Article Online
DOI: 10.1039/C7TA00366H

Graphical abstracts

Recent Advances in Perovskite Solar Cells: Efficiency, Stability and Lead-free Perovskite

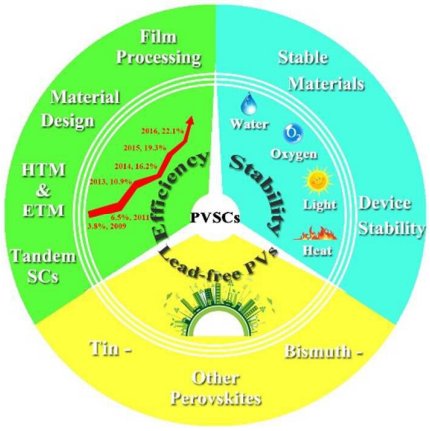

In this review, we first highlight recent progress in high performance perovskite solar cells (PVSCs) with discussion about fabrication methods and PVSCs based tandem solar cells. Further, stability issue of PVSCs and strategies to improve material and device stability are discussed, and finally, summary of recent progress of lead-free perovskites are presented.